IEEE Access
Multidisciplinary ⋮ Rapid Review ⋮ Open Access Journal

Received March 13, 2021, accepted March 30, 2021, date of publication April 13, 2021, date of current version June 3, 2021.

Digital Object Identifier 10.1109/ACCESS.2021.3072952

Design of Morlet Wavelet Neural Network for Solving a Class of Singular Pantograph Nonlinear Differential Models

KASHIF NISAR[1], (Senior Member, IEEE), ZULQURNAIN SABIR[2], MUHAMMAD ASIF ZAHOOR RAJA[3,4], AG. ASRI AG. IBRAHIM[1], (Member, IEEE), FEVZI ERDOGAN[5], MUHAMMAD REAZUL HAQUE[6], (Member, IEEE), JOEL J. P. C. RODRIGUES[7,8], (Fellow, IEEE), AND DANDA B. RAWAT[9], (Senior Member, IEEE)

[1]Faculty of Computing and Informatics, Universiti Malaysia Sabah, Kota Kinabalu 88400, Malaysia
[2]Department of Mathematics, Hazara University, Mansehra 21120, Pakistan
[3]Department of Electrical and Computer Engineering, COMSATS University Islamabad at Attock, Attock 43600, Pakistan
[4]Future Technology Research Center, National Yunlin University of Science and Technology, Yunlin 64002, Taiwan
[5]Department of Mathematics, Yuzuncu Yil University, 65080 Van, Turkey
[6]Faculty of Computing and Informatics, Multimedia University, Cyberjaya 63100, Malaysia
[7]Post-Graduation Program in Electrical Engineering, Federal University of Piauí (UFPI), Teresina 64049-550, Brazil
[8]Covilhã Delegation, Instituto de Telecomunicações, 6201-001 Covilhã, Portugal
[9]Data Science and Cybersecurity Center, Department of Electrical Engineering and Computer Science, Howard University, Washington, DC 20059, USA

Corresponding author: Kashif Nisar (kashif@ums.edu.my)

This work was supported in part by the University Malaysia Sabah, Malaysia, in part by the FCT/MCTES through national funds and when applicable co-funded EU funds under Project UIDB/50008/2020, and in part by the Brazilian National Council for Scientific and Technological Development—CNPq, under Grant 313036/2020-9.

ABSTRACT The aim of this study is to design a layer structure of feed-forward artificial neural networks using the Morlet wavelet activation function for solving a class of pantograph differential Lane-Emden models. The Lane-Emden pantograph differential equation is one of the important kind of singular functional differential model. The numerical solutions of the singular pantograph differential model are presented by the approximation capability of the Morlet wavelet neural networks (MWNNs) accomplished with the strength of global and local search terminologies of genetic algorithm (GA) and interior-point algorithm (IPA), i.e., MWNN-GAIPA. Three different problems of the singular pantograph differential models have been numerically solved by using the optimization procedures of MWNN-GAIPA. The correctness of the designed MWNN-GAIPA is observed by comparing the obtained results with the exact solutions. The analysis for 3, 6 and 60 neurons are also presented to check the stability and performance of the designed scheme. Moreover, different statistical analysis using forty number of trials is presented to check the convergence and accuracy of the proposed MWNN-GAIPA scheme.

INDEX TERMS Pantograph, singular, artificial neural networks, genetic algorithms, neuron analysis, interior-point algorithm.

I. INTRODUCTION

Pantograph equation is one of the specific form of the functional differential system that contain proportional delays. Ockendon and Tayler (1971) [1] introduced first time the word ''pantograph'' by working on the project named as a current collection using the pantograph head of an electric'' [1]. The pantograph differential equations have many applications in the area of theory [2], cell-growth biological based models [3] and control system [4]. The pantograph differential equations have been solved by many techniques, some of them are intelligent networks [5], Chebyshev spectral scheme [6], spectral tau scheme [7], multidimensional homotopy optimal asymptotic scheme [8], Genocchi operational based matrix scheme [9], least-squares-Epsilon-Ritz scheme [10], Taylor operation scheme [11], Galerkin multi-wavelets scheme [12], heuristic computing approach [13], Sinc numerical scheme [14], Laplace

The associate editor coordinating the review of this manuscript and approving it for publication was Yudong Zhang.

transform scheme [15], spectral collocation approach [16], multistep block method [17], Legendre Tau computational scheme [18] and Euler–Maruyama scheme [19].

This singular study is considered very significant due to its extensive applications in radiators cooling, dusty fluids, classical/quantum-based mechanics, models of gas cloud and galaxies [20]–[22]. It is not easy and always a big challenge for the research community to solve the Lane-Emden form of the model due to singular-point at the origin. The general form of the singular Lane-Emden equation is given as [23]–[25]:

$$\begin{cases} h''(\tau) + \dfrac{\Omega}{\tau} h'(\tau) + g(h) = f(\tau), \\ h(0) = I, \;\; h'(0) = 0, \end{cases} \tag{1}$$

where I is a constant, $\Omega \geq 1$ represents a shape factor, the singularity arises at $\tau = 0$. The present study is related to solve a singular pantograph (proportional delay with parameter a) differential model and is given as [26]:

$$\begin{cases} a\,h''(a\tau) + \dfrac{\Omega}{\tau} h'(a\tau) + g(h) = f(\tau), \\ h(0) = I, \;\; h'(0) = 0. \end{cases} \tag{2}$$

The above equation shows a singular form of the pantograph differential model, the multiple delays are noticed in the 1st and 2nd terms.

The aim of the present study is to solve the singular pantograph differential model of second kind by designing a layer structure of feed-forward artificial neural networks using the Morlet wavelet activation function, while the optimization task is accomplished with the strength of global and local search terminologies of genetic algorithm (GA) and interior-point algorithm (IPA), i.e., MWNN-GAIPA. The stochastic procedures have been implemented to solve various problems like nonlinear SIR system of dengue fever [27], prey-predator models [28], infectious disease model [29], rotational dynamics of nanofluid flow over a stretching sheet with thermal radiation [30], HIV infection spread model [31], nonlinear periodic singular boundary value problems [32], forecasting of the financial market [33], nonlinear multi-singular systems [34], singular third kind of differential model [35], COVID-19 dynamical SITR system [36] and heat conduction dynamics based human head system [37]. These cited inspirations motivated the authors to present the design of MWNN-GAIPA for solving a class of singular pantograph differential model. Potential salient topographies of proposed integrated heuristics of MWNN-GAIPA in terms of contribution and innovative insights are presented as follows:

- Novel design of integrated heuristic MWNN-GAIPA is presented through layer structure of feed-forward ANNs involving Morlet-Wavelet activation function for the hidden neurons to solving a class of singular pantograph differential models while the optimization is accomplished with the strength of respective global and local search terminologies of GA and IPA.
- The correctness of the designed MWNN-GAIPA is consistently observed by comparing the proposed and exact solutions for solving different problems of the singular pantograph models.
- The designed MWNN-GAIPA is implemented viably to solve the singular pantograph models via 3, 6 and 10 neurons based networks with reasonable accuracy on absolute error (AE), root mean square error (R.MSE), Theil's inequality coefficients (TIC) and variance account for (VAF) indices on single and multiple runs to validate the performance.
- Beside the precise results of the singular pantograph differential model, robustness, simple understanding of the concept, smooth processes wit implementation and wide-ranging applicability are well-regarded perks of integration heuristic MWNN-GAIPA.

The remaining paper is organized as: Section 2 describes the design of MWNN-GAIPA in detail. Performance operators are described in Section 3. Simulations are performed in Section 4. future research reports are described in the last conclusions Section.

II. METHODOLOGY: MWNNS

The ability to design the MWNNs for providing the stable, reliable and steady solutions in various fields. The mathematical form of the singular pantograph differential model is stated with feed-forward MWNNs in the form of designing solutions along with their derivatives are written as:

- The design of fitness function is presented using the differential system and the boundary conditions.
- The optimal form of GAIPA is provided based on the pseudocode and preliminary material.

A. MWNNS MODELING

The mathematical form of the MWNNs for solving the singular pantograph differential model is presented in this section. In the below system, $\hat{h}(\tau)$ represents the approximate form of the results.

$$\begin{aligned} \hat{h}(\tau) &= \sum_{k=1}^{s} u_k l(w_k \tau + v_k), \\ \hat{h}^{(n)} &= \sum_{k=1}^{s} u_k l^{(n)}(w_k \tau + v_k) \end{aligned} \tag{3}$$

In the equation (3), s indicates the number of neurons, $\boldsymbol{W} = [\boldsymbol{u}, \boldsymbol{w}, \boldsymbol{v}]$ represents the unidentified weight vector, i.e., $\boldsymbol{u} = [u_1, u_2, \ldots, u_s]$, $\boldsymbol{w} = [w_1, w_2, \ldots, w_s]$ and $\boldsymbol{v} = [v_1, v_2, \ldots, v_s]$. The MWNNs are not designed nor implemented before to solve the singular pantograph differential model. The mathematical form of the MW function is given as [38]–[41]:

$$l(\tau) = \cos(1.75\tau)\, e^{(-0.5\tau^2)}. \tag{4}$$

The updated form of the system (3) using the above MW function is given as (5), shown at the bottom of the next page.

A fitness function (E) is written as:

$$E = E_1 + E_2 \tag{6}$$

where E_1 and E_2 represent an unsupervised error using the differential system and boundary conditions, written as:

$$E_1 = \frac{1}{N}\sum_{k=1}^{N}\left(ah''(a\tau_k) + \frac{\Omega}{\tau_k}h'(a\tau_k) + g(h_k) - f_k\right), \tag{7}$$

where $h_k = h(\tau_k)$, $f_k = f(\tau_k)$, $g_k = g(\tau_k)$ and $\tau_k = kh$

$$E_2 = \frac{1}{2}\left(\hat{h}_0 - I_1\right)^2 + \frac{1}{2}\left(\hat{h}'_0\right)^2. \tag{8}$$

B. OPTIMIZATION PROCESS: GAIPA

In this section, the optimization procedures of the hybrid of GA-IPAIPA to solve each problem of the singular pantograph differential model are described.

Genetic Algorithm is known as first stochastic population-based optimization algorithm proposed in the literature. GA work through its well-known operators called selection, mutation and crossover. It can be applied to optimize both constrained and unconstrained types of problems. Recently, GA is applied in many famous applications of heart diagnosis system [42], nonlinear electric circuit models [43], nonlinear astrophysics based singular system [44], Painlevé equation-II based nonlinear optic models [45], prediction model of air blast [46], Thomas Fermi model [47], and monorail vehicle system [48]. These potential applications of GA inspired the authors to solve the singular pantograph differential model to attain the decision variables of MWNNs.

Interior-point algorithm is a local search optimization procedure work to solve stiff, complicated and convex models. Recently, IPA is implemented in image renewal [49], state estimation of power system [50], nested-constraint resource allocation models [51] and PDE-constrained of risk-averse based optimization models [52]. The sluggishness and laziness of GA procedure can be controlled by using the hybridization processes with IPA based on the optimum performance. The hybridization detail of GAIPA is given in Table 1.

III. PERFORMANCE PROCEDURES

The statistical performances based on R.MSE, VAF, TIC and semi-interquartile range (S.I.R) along with global measures of RMSE, VAF and TIC have been provided. The mathematical measures of these performances are given as:

$$RMSE = \sqrt{\frac{1}{s}\sum_{i=1}^{s}\left(h_i - \hat{h}_i\right)^2}, \tag{9}$$

$$\begin{cases} VAF = \left(1 - \dfrac{\text{var}\left(h_i - \hat{h}_i\right)}{\text{var}\left(h_i\right)}\right) \times 100, \\ \text{E-VAF} = \left[|\text{VAF-100}|\right], \end{cases} \tag{10}$$

$$TIC = \frac{\sqrt{\frac{1}{s}\sum_{i=1}^{s}\left(h_i - \hat{h}_i\right)^2}}{\left(\sqrt{\frac{1}{s}\sum_{i=1}^{s}h_i^2} + \sqrt{\frac{1}{s}\sum_{i=1}^{s}\hat{h}_i^2}\right)}, \tag{11}$$

$$\begin{cases} S.I.R = \dfrac{1}{2}\left(q_3 - q_1\right), \\ q_1 = 1^{st}\text{ quartile}, \quad q_3 = 3^{rd}\text{ quartile}. \end{cases} \tag{12}$$

IV. NUMERICAL PERFORMANCES

In this section, the comprehensive detail of each problem of the singular pantograph differential model is provided.

A. PROBLEM I

Consider a singular nonlinear pantograph differential equation is obtained by taking $a = 0.5$ and $\Omega = 3$ in equation (2) as :

$$\begin{cases} \dfrac{1}{2}h''(\dfrac{1}{2}\tau) + \dfrac{3}{\tau}h'(\dfrac{1}{2}\tau) + h^2 = 1 + 3\tau^2 + 2\tau^4 + \tau^8, \\ h(0) = 1, \quad h'(0) = 0. \end{cases} \tag{13}$$

The exact solution of Eq. (13) is $\tau^4 + 1$ and the fitness function becomes as:

$$E = \frac{1}{N}\sum_{m=1}^{N}\left(\begin{array}{l}\dfrac{1}{2}\hat{h}''(\dfrac{1}{2}\tau_m) + \dfrac{3}{\tau_m}\hat{h}'(\dfrac{1}{2}\tau_m) \\ +\hat{h}_m^2 - 1 - 3\tau_m^2 - 2\tau_m^4 - \tau_m^8\end{array}\right)^2 + \frac{1}{2}\left((\hat{h}_0 - 1)^2 + \left(\hat{h}'_0\right)^2\right). \tag{14}$$

B. PROBLEM II

Consider a singular nonlinear pantograph differential equation with trigonometric function is obtained by taking

$$\begin{aligned} \hat{h}(\tau) &= \sum_{k=1}^{s} u_k \cos\left(1.75(w_k\tau + v_k)\right) e^{-0.5(w_k\tau+v_k)^2}, \\ \hat{h}'(\tau) &= \sum_{k=1}^{s}\left(-u_k w_k e^{-0.5(w_k\tau+m_k)^2}\right)\left(\sin\left(1.75\left(w_k\tau + v_k\right)\right) + 1.75\left(w_k\tau + v_k\right)\cos\left(1.75\left(w_k\tau + v_k\right)\right)\right), \\ \hat{h}''(\tau) &= \sum_{i=1}^{s} -u_k w_k^2 e^{-\frac{1}{2}(w_k\tau+v_k)^2}\left(\begin{array}{l}3.0625\cos\left(1.75(w_k\tau + v_k)\right) + 3.5(w_k\tau + v_k)\sin\left(1.75(w_k\tau + v_k)\right) \\ +\left(-1 + (w_k\tau + v_k)^2\right)\cos\left(1.75(w_k\tau + v_k)\right)\end{array}\right), \end{aligned} \tag{5}$$

TABLE 1. Optimization process using MWNN-GAIPA for solving singular pantograph model.

"GA" start
- i) **Inputs:** The chromosomes are selected with same number of entries of the network as: $W=[u,w,v]$
- ii) **Population:** The weight vectors are defined as: $u=[u_1,u_2,u_3,\ldots,u_s]$, $w=[w_1,w_2,w_3,\ldots,w_s]$ and $v=[v_1,v_2,v_3,\ldots,v_s]$.
- iii) **Output:** GA best values are represented as: $W_{B\text{-}GA}$
- iv) **Initialization:** Form "W" to represent a 'chromosome'. Set of weight vector is functional to the primary population. Adjust the 'declaration' and 'Generation' values for [gaoptimset] & [GA].
- v) **Fitness formulations:** Fine-tune the "**E**" that is a FIT value in population using the Eqs (6)-(8).
- vi) **Termination method:** Terminate, if one of the below condition obtains
  - [FIT=10^{-20}], [StallLimit=125], [PopulationSize=240],
  - [(TolCon)= 10^{-19}], [(TolFun)=10^{-18}], [Generations =135],
  - Other values: default.

  Move to **(storage)** to accomplish the standards of termination.
- vii) **Ranking:** In FIT values, rank each (W) in the Population
- viii) **Reproduction:** (Selection=Selection uniform), (Mutations):(mutationadaptfeasible), (Crossover):(crossoverheuristic), (Elitism): For population best values, continue FIT valuation
- iX) **Storage:** Store $W_{B\text{-}GA}$, Generations, function counts, time, E and for the current of 'GA'.

'GA' Ends

IPA Starts
- i) **Inputs:** Start point: $W_{B\text{-}GA}$
- ii) **Output:** GAIPA best values: W_{GAIPA}.
- iii) **Initialize:** Take W_{BGA}, iterations, assignments, Bounded restraints and other values.
- iv) **Terminate:** Stop, if [MaxFunEvals= 285000], [TolX=10^{-22}], [E=10^{-20}], [Iterations = 500], [TolFun=10^{-22}], [TolCon=10^{-22}], While [Stop] do steps v and vi
- v) **Fitness formulations:** Compute E, W by using (6)-(8).
- vi) **Adjustments:** Invoke (fmincon) for IPA. Regulate (W) for IPA. Compute E of modified 'W' using Eqs. (6)-(8).
- vii) **Accumulate:** Regulate 'W_{GAIPA}', E, function counts, time and generations for current execution of IPA.

End of IPA

Data Generations: Repeat IPA for 40 times for 3, 6 and 10 neurons to get a broaden dataset of the optimization for using the statistical clarifications

$\alpha = 1/2$ and $\Omega = 3$ in equation (2) as:

$$\begin{cases} \frac{1}{2}h''(\frac{1}{2}\tau)+\frac{3}{\tau}h'(\frac{1}{2}\tau)+h^{-2}=\sec^2(\tau)- \\ \frac{3}{\tau}\sin\left(\frac{1}{2}\tau\right)-\frac{1}{2}\cos\left(\frac{1}{2}\tau\right), \\ h(0)=1,\ h'(0)=0. \end{cases} \tag{15}$$

The exact solution of Eq. (15) is $\cos(\tau)$ and the fitness function becomes as:

$$E=\frac{1}{N}\sum_{m=1}^{N}\left(\begin{array}{l}\frac{1}{2}\hat{h}''(\frac{1}{2}\tau_m)+\frac{3}{\tau_m}\hat{h}'(\frac{1}{2}\tau_m) \\ +\hat{h}_m^{-2}+\frac{3}{\tau}\sin\left(\frac{1}{2}\tau_m\right)- \\ \sec^2(\tau_m)+\frac{1}{2}\cos\left(\frac{1}{2}\tau_m\right)\end{array}\right)^2 +\frac{1}{2}\left((\hat{h}_0-1)^2+\left(\hat{h}'_0\right)^2\right). \tag{16}$$

C. PROBLEM III

Consider a singular nonlinear pantograph differential equation with exponential function is obtained by taking $\alpha = 1/2$ and $\Omega = 3$ in equation (2) as:

$$\begin{cases} \frac{1}{2}h''(\frac{1}{2}\tau)+\frac{3}{\tau}h'(\frac{1}{2}\tau)+e^h=\frac{15}{4}\tau+e^{1+\tau^3}, \\ h(0)=1,\ h'(0)=0. \end{cases} \tag{17}$$

The exact solution of Eq. (17) is $1+\tau^3$ and the fitness function becomes as:

$$E=\frac{1}{N}\sum_{m=1}^{N}\left(\begin{array}{l}\frac{1}{2}\hat{h}''(\frac{1}{2}\tau_m)+\frac{3}{\tau_m}\hat{h}'(\frac{1}{2}\tau_m)+ \\ e^{\hat{h}_m}-\frac{15}{4}\tau_m-e^{1+\tau_m^3}\end{array}\right)^2 +\frac{1}{2}\left((\hat{h}_0-1)^2+\left(\hat{h}'_0\right)^2\right). \tag{18}$$

The optimization of all problems based MWNN-GAIPA for forty independent implementations to measure the system parameter. The set of best weight vectors is accessible to validate the solutions of the singular pantograph differential model are provided in systems (19-21) for 3 neurons, equations (22-24) for 6 neurons and equations (25-27) for 10 neurons. The mathematical illustrations of the proposed

system for 3, 6 and 10 neurons are provided as:

$$\begin{aligned}\hat{y}_{P-\mathrm{I}}(\tau) = {} & 1.1185\cos\left(1.75(1.8307\tau - 3.3665)\right) \\ & \times e^{-0.5(1.8307\tau-3.3665)^2} \\ & +1.1307\cos\left(1.75(0.0945\tau - 0.2158)\right) \\ & \times e^{-0.5(0.0945\tau-0.2158)^2} \\ & -8.7957\cos\left(1.75(-1.370\tau + 3.3376)\right) \\ & \times e^{-0.5(-1.370\tau+3.3376)^2}, \end{aligned} \tag{19}$$

$$\begin{aligned}\hat{y}_{P-\mathrm{II}}(\tau) = {} & 0.9212\cos\left(1.75(0.7290\tau + 1.3776)\right) \\ & \times e^{-0.5(0.7290\tau+1.3776)^2} \\ & +4.5861\cos\left(1.75(0.0245\tau + 1.0652)\right) \\ & \times e^{-0.5(0.0245\tau+1.0652)^2} \\ & -6.9918\cos\left(1.75(0.3865\tau + 1.3825)\right) \\ & \times e^{-0.5(0.3865\tau+1.3825)^2}, \end{aligned} \tag{20}$$

$$\begin{aligned}\hat{h}_{P-\mathrm{III}}(\tau) = {} & -7.6628\cos\left(1.75(1.2005\tau - 3.0114)\right) \\ & \times e^{-0.5(1.2005\tau-3.0114)^2} \\ & +8.4815\cos\left(1.75(14.1955\tau + 6.3650)\right) \\ & \times e^{-0.5(14.195\tau+6.365)^2} \\ & -19.999\cos\left(1.75(-19.997\tau - 4.591)\right) \\ & \times e^{-0.5(-19.997\tau-4.591)^2}, \end{aligned} \tag{21}$$

$$\begin{aligned}\hat{h}_{P-\mathrm{I}}(\tau) = {} & -6.1962\cos\left(1.75(-1.384\tau + 3.3573)\right) \\ & \times e^{-0.5(-1.384\tau+3.357)^2} \\ & -0.0340\cos\left(1.75(-3.419\tau - 3.094)\right) \\ & \times e^{-0.5(-3.4199\tau-3.0948)^2} \\ & +4.0022\cos\left(1.75(-2.140\tau - 4.492)\right) \\ & \times e^{-0.5(-2.1402\tau-4.4924)^2} + \ldots. \\ & -3.9678\cos\left(1.75(0.0545\tau + 1.2277)\right) \\ & \times e^{-0.5(0.0545\tau+1.2277)^2}, \end{aligned} \tag{22}$$

$$\begin{aligned}\hat{h}_{P-\mathrm{II}}(\tau) = {} & -6.5857\cos\left(1.75(4.3869\tau - 7.2459)\right) \\ & \times e^{-0.5(4.3869\tau-7.2459)^2} \\ & -19.984\cos\left(1.75(-19.98\tau - 4.8954)\right) \\ & \times e^{-0.5(-19.984\tau-4.895)^2} \\ & -3.4919\cos\left(1.75(0.4386\tau + 1.4042)\right) \\ & \times e^{-0.5(0.4386\tau+1.4042)^2} + \ldots. \\ & +5.5609\cos\left(1.75(-2.805\tau - 6.1770)\right) \\ & \times e^{-0.5(-2.805\tau-6.177)^2}, \end{aligned} \tag{23}$$

$$\begin{aligned}\hat{h}_{P-\mathrm{III}}(\tau) = {} & 19.8820\cos\left(1.75(-7.531\tau + 10.526)\right) \\ & \times e^{-0.5(-7.531\tau+10.526)^2} \\ & +19.9904\cos\left(1.75(-1.200\tau - 2.9950)\right) \\ & \times e^{-0.5(-1.200\tau-2.9950)^2} \\ & +19.9904\cos\left(1.75(2.1789\tau - 2.9950)\right) \\ & \times e^{-0.5(2.1789\tau-2.9950)^2} + \ldots. \\ & +19.9904\cos\left(1.75(5.7162\tau + 2.9950)\right) \\ & \times e^{-0.5(5.7162\tau+2.9950)^2}, \end{aligned} \tag{24}$$

$$\begin{aligned}\hat{h}_{P-\mathrm{I}}(\tau) = {} & 1.9350\cos\left(1.75(1.4911\tau - 3.0408)\right) \\ & \times e^{-0.5(1.4911\tau-3.0408)^2} \\ & +1.2213\cos\left(1.75(0.5620\tau - 1.4487)\right) \\ & \times e^{-0.5(0.5620\tau-1.4487)^2} \\ & +1.1784\cos\left(1.75(-0.801\tau + 1.6328)\right) \\ & \times e^{-0.5(-0.801\tau+1.6328)^2} + \ldots. \\ & +0.6803\cos\left(1.75(-0.935\tau + 0.9500)\right) \\ & \times e^{-0.5(-0.935\tau+0.9500)^2}, \end{aligned} \tag{25}$$

$$\begin{aligned}\hat{h}_{P-\mathrm{II}}(\tau) = {} & -0.2234\cos\left(1.75(0.1656\tau + 0.5931)\right) \\ & \times e^{-0.5(0.1656\tau+0.5931)^2} \\ & +0.2954\cos\left(1.75(0.7497\tau + 0.4631)\right) \\ & \times e^{-0.5(0.7497\tau+0.4631)^2} \\ & +0.3447\cos\left(1.75(-0.246\tau + 0.656)\right) \\ & \times e^{-0.5(-0.2465\tau+0.6560)^2} + \ldots. \\ & +1.2298\cos\left(1.75(-0.065\tau + 0.713)\right) \\ & \times e^{-0.5(-0.0653\tau+0.7138)^2}, \end{aligned} \tag{26}$$

$$\begin{aligned}\hat{h}_{P-\mathrm{III}}(\tau) = {} & -0.3763\cos\left(1.75(-1.304\tau + 0.3991)\right) \\ & \times e^{-0.5(-1.304\tau+0.3991)^2} \\ & -3.7109\cos\left(1.75(-0.533\tau - 1.5608)\right) \\ & \times e^{-0.5(-0.533\tau-1.5608)^2} \\ & -0.3684\cos\left(1.75(-0.560\tau - 2.0094)\right) \\ & \times e^{-0.5(-0.560\tau-2.0094)^2} + \ldots. \\ & -8.6956\cos\left(1.75(1.2298\tau - 3.4399)\right) \\ & \times e^{-0.5(1.2298\tau-3.4399)^2}. \end{aligned} \tag{27}$$

For solving each problem of the singular pantograph differential model, the MWNN-GAIPA optimization performance for 40 independent implementations using 3, 6 and 10 neurons are provided. Fig. 1 presents the 3, 6 and 10 neurons based on the equations (19-27) to get the best weights of the approximate results of the MWNN-GAIPAS.

Fig. 2 shows the comparison of the obtained results with the exact solutions for solving all problems of the singular pantograph differential model using 3, 6 and 10 neurons. The exactly overlapping of the results for 3, 6 and 10 neurons enhance the performance of the designed MWNN-GAIPA for solving singular pantograph differential model.

Table 2-4 shows the performances based on Minimum (Min), Mean, Median (Med), standard deviation (SD) and S.I.R values for 3, 6 and 10 neurons using the designed MWNN-GAIPA to solve the singular pantograph differential model. The values-based Min, Mean, Med, SD and S.I.R for Problems I-III lie in good ranges. These observed small values based on the mention gages for Problems I-III of the singular pantograph differential model using 3, 6 and 10 neurons indicate the correctness of the MWNN-GAIPA scheme.

The plots of AE for each problem of the singular pantograph differential model for 3, 6 and 10 neurons are drawn in Fig. 3(a), 3(b) and 3(c), respectively. The AE values

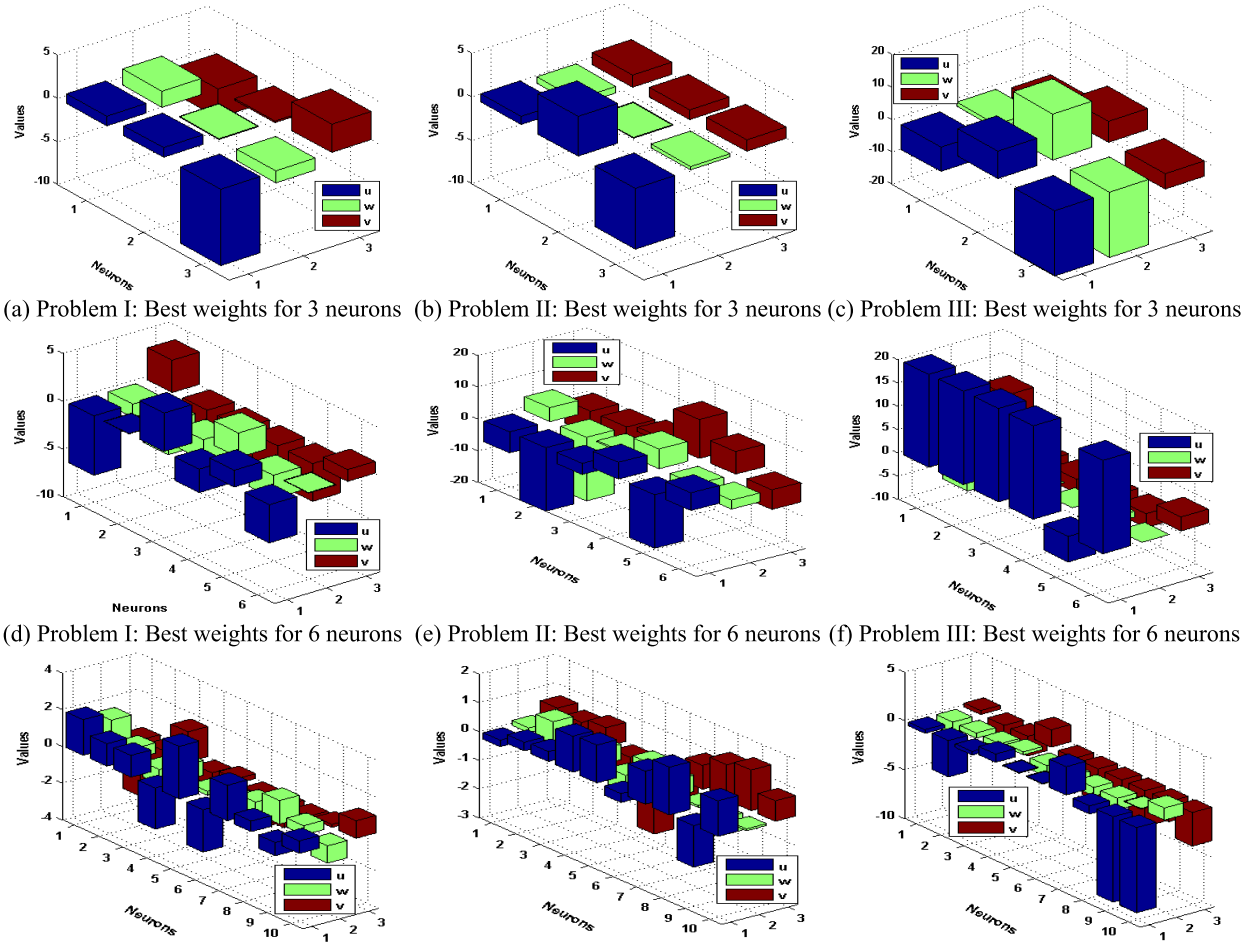

(a) Problem I: Best weights for 3 neurons (b) Problem II: Best weights for 3 neurons (c) Problem III: Best weights for 3 neurons

(d) Problem I: Best weights for 6 neurons (e) Problem II: Best weights for 6 neurons (f) Problem III: Best weights for 6 neurons

(g) Problem I: Best weights for 10 neurons(h) Problem II: Best weights for 10 neurons(i) Problem III: Best weights for 3 neurons

FIGURE 1. **Best weight through MWNN-GAIPA for each problem of the singular pantograph differential model using 3, 6 and 10 neurons (a)-(i).**

TABLE 2. **The statics performances of MWNN-GAIPA for the singular prediction differential model using 3 neurons.**

	Mode	$\hat{h}(\tau)$									
		0	**0.1**	**0.2**	**0.3**	**0.4**	**0.5**	**0.6**	**0.7**	**0.8**	**0.9**	**1**
P-I	Min	1×10^{-05}	6×10^{-05}	1×10^{-04}	7×10^{-05}	1×10^{-04}	2×10^{-04}	1×10^{-05}	4×10^{-04}	3×10^{-03}	3×10^{-03}	1×10^{-03}
	Mean	7×10^{-01}	8×10^{-01}	8×10^{-01}	8×10^{-01}	8×10^{-01}	8×10^{-01}	9×10^{-01}	1×10^{-02}	1×10^{-01}	2×10^{-01}	3×10^{-01}
	SD	3×10^{-01}	3×10^{-01}	3×10^{-01}	3×10^{-01}	3×10^{-01}	3×10^{-01}	4×10^{-01}	7×10^{-02}	1×10^{-01}	2×10^{-01}	2×10^{-01}
	Med	9×10^{-01}	1×10^{-01}	9×10^{-01}	9×10^{-01}	9×10^{-01}	9×10^{-01}	1×10^{-01}	1×10^{-02}	1×10^{-01}	2×10^{-01}	4×10^{-02}
	S.I.R	5×10^{-02}	5×10^{-02}	5×10^{-02}	5×10^{-02}	6×10^{-02}	8×10^{-02}	1×10^{-01}	5×10^{-02}	1×10^{-02}	1×10^{-02}	2×10^{-02}
P-II	Min	1×10^{-05}	4×10^{-06}	1×10^{-05}	1×10^{-05}	1×10^{-05}	1×10^{-05}	7×10^{-06}	7×10^{-06}	2×10^{-05}	4×10^{-05}	3×10^{-05}
	Mean	1×10^{-01}	2×10^{-01}	2×10^{-01}	2×10^{-01}	2×10^{-01}	2×10^{-01}	2×10^{-01}	2×10^{-01}	3×10^{-01}	2×10^{-01}	2×10^{-01}
	SD	3×10^{-01}	4×10^{-01}	4×10^{-01}	5×10^{-01}	5×10^{-01}	5×10^{-01}	5×10^{-01}	5×10^{-01}	5×10^{-01}	4×10^{-01}	4×10^{-01}
	Med	1×10^{-03}	2×10^{-03}	1×10^{-03}	2×10^{-03}	4×10^{-03}	1×10^{-02}	1×10^{-02}	1×10^{-02}	1×10^{-02}	7×10^{-03}	9×10^{-03}
	S.I.R	1×10^{-02}	1×10^{-02}	1×10^{-02}	1×10^{-02}	1×10^{-02}	1×10^{-02}	2×10^{-02}	7×10^{-02}	1×10^{-01}	3×10^{-02}	2×10^{-01}
P-III	Min	4×10^{-07}	1×10^{-05}	5×10^{-06}	1×10^{-05}	6×10^{-06}	4×10^{-06}	2×10^{-05}	1×10^{-04}	7×10^{-06}	4×10^{-04}	3×10^{-04}
	Mean	6×10^{-01}	6×10^{-01}	6×10^{-01}	6×10^{-01}	6×10^{-01}	5×10^{-01}	5×10^{-01}	5×10^{-01}	1×10^{-02}	7×10^{-01}	1×10^{-02}
	SD	4×10^{-01}	4×10^{-01}	4×10^{-01}	4×10^{-01}	4×10^{-01}	4×10^{-01}	4×10^{-01}	7×10^{-01}	4×10^{-02}	1×10^{-02}	4×10^{-02}
	Med	9×10^{-01}	9×10^{-01}	9×10^{-01}	8×10^{-01}	8×10^{-01}	8×10^{-01}	7×10^{-01}	5×10^{-01}	5×10^{-01}	5×10^{-01}	4×10^{-01}
	S.I.R	5×10^{-01}	5×10^{-01}	5×10^{-01}	5×10^{-01}	4×10^{-01}	4×10^{-01}	4×10^{-01}	3×10^{-01}	3×10^{-01}	2×10^{-01}	2×10^{-01}

are observed for 3 neurons for problems I, II and III lie around 10^{-03}-10^{-05}, 10^{-05}-10^{-06} and 10^{-04}-10^{-06}, respectively. For 6 numbers of neurons, the AE values for problems I, II and III lie around 10^{-03}-10^{-06}, 10^{-05}-10^{-06} and 10^{-04}-10^{-07}, respectively. For 10 neurons, the values of AE for problems I, II and III found around 10^{-04}-10^{-08}, 10^{-04}-10^{-06} and 10^{-04}-10^{-07}, respectively. One can observe on the behalf of AE for each problem of the singular pantograph

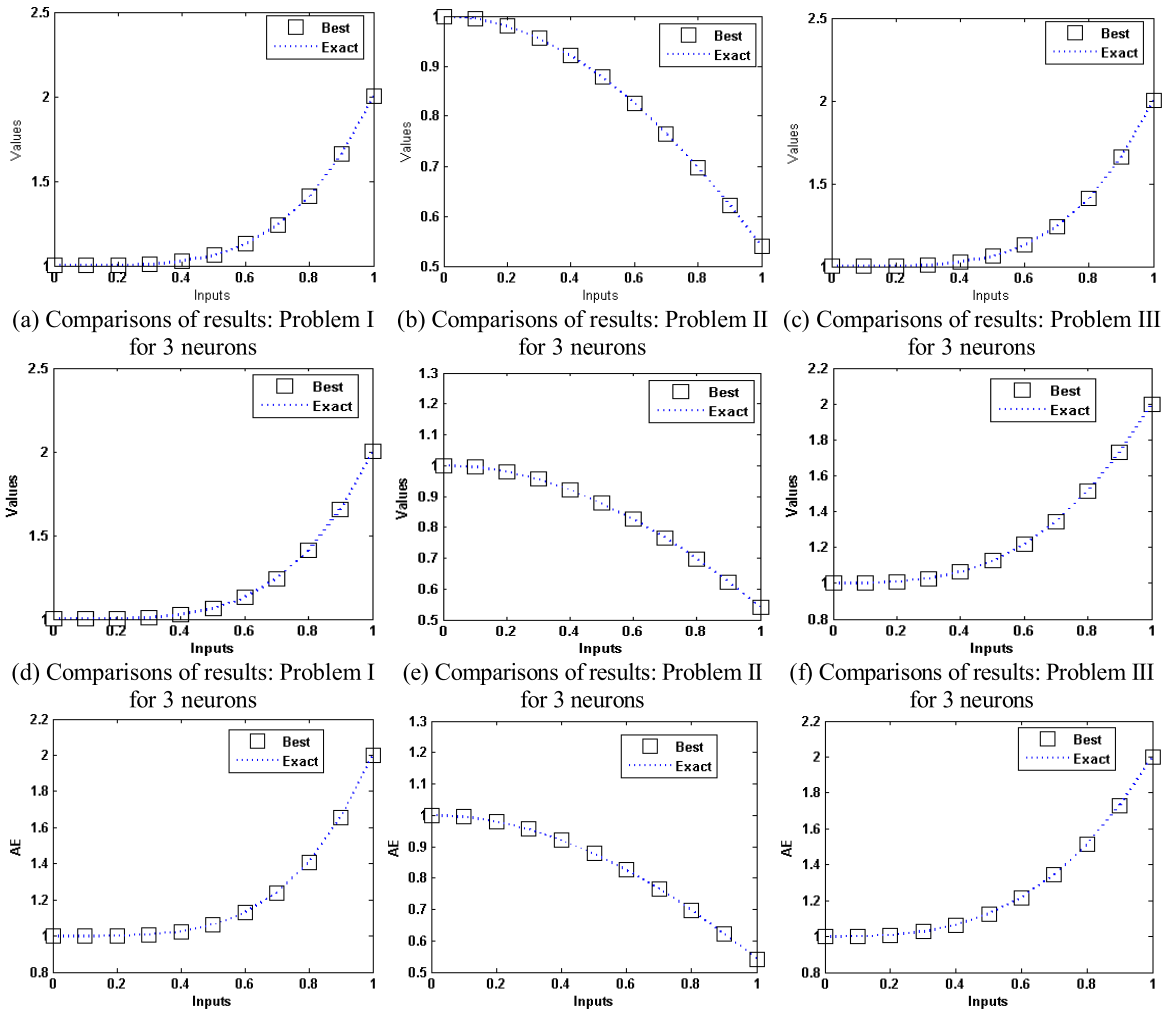

(a) Comparisons of results: Problem I for 3 neurons (b) Comparisons of results: Problem II for 3 neurons (c) Comparisons of results: Problem III for 3 neurons

(d) Comparisons of results: Problem I for 3 neurons (e) Comparisons of results: Problem II for 3 neurons (f) Comparisons of results: Problem III for 3 neurons

(g) Comparisons of results: Problem I for 3 neurons (h) Comparisons of results: Problem II for 3 neurons (i) Comparisons of results: Problem III for 3 neurons

FIGURE 2. **Result comparison based on best and exact solutions through MWNN-GAIPA for each problem of the singular pantograph differential model using 3, 6 and 10 neurons (a)-(i).**

TABLE 3. **The statics performances of MWNN-GAIPA for the singular prediction differential model using 6 neurons.**

	Mode	$\hat{h}(\tau)$										
		0	**0.1**	**0.2**	**0.3**	**0.4**	**0.5**	**0.6**	**0.7**	**0.8**	**0.9**	**1**
P-I	Min	2×10^{-06}	1×10^{-02}	1×10^{-01}	2×10^{-01}	2×10^{-01}	3×10^{-01}	3×10^{-01}	1×10^{-02}	2×10^{-03}	2×10^{-02}	5×10^{-02}
	Mean	3×10^{-01}	4×10^{-01}	5×10^{-01}	6×10^{-01}	7×10^{-01}	8×10^{-01}	1×10^{-02}	1×10^{-02}	1×10^{-01}	2×10^{-02}	3×10^{-02}
	SD	4×10^{-01}	4×10^{-01}	4×10^{-01}	4×10^{-01}	4×10^{-01}	4×10^{-01}	7×10^{-01}	1×10^{-02}	1×10^{-02}	2×10^{-01}	2×10^{-01}
	Med	4×10^{-02}	1×10^{-01}	2×10^{-01}	2×10^{-01}	3×10^{-01}	4×10^{-01}	6×10^{-01}	1×10^{-01}	1×10^{-02}	9×10^{-01}	2×10^{-01}
	S.I.R	4×10^{-01}	4×10^{-01}	4×10^{-01}	4×10^{-01}	4×10^{-01}	4×10^{-01}	4×10^{-01}	9×10^{-01}	1×10^{-02}	1×10^{-02}	2×10^{-02}
P-II	Min	2×10^{-02}	1×10^{-01}	4×10^{-01}	6×10^{-01}	5×10^{-01}	3×10^{-01}	2×10^{-01}	4×10^{-02}	2×10^{-03}	3×10^{-02}	2×10^{-02}
	Mean	9×10^{-01}	7×10^{-01}	7×10^{-01}	6×10^{-01}	5×10^{-01}	4×10^{-01}	3×10^{-01}	2×10^{-01}	3×10^{-01}	3×10^{-01}	4×10^{-01}
	SD	2×10^{-01}	2×10^{-01}	1×10^{-01}	1×10^{-02}	1×10^{-01}	2×10^{-01}	3×10^{-01}	3×10^{-01}	9×10^{-01}	4×10^{-01}	4×10^{-01}
	Med	1×10^{-02}	9×10^{-01}	7×10^{-01}	6×10^{-01}	5×10^{-01}	4×10^{-01}	2×10^{-01}	1×10^{-01}	2×10^{-02}	1×10^{-01}	3×10^{-01}
	S.I.R	1×10^{-04}	1×10^{-04}	1×10^{-04}	2×10^{-04}	4×10^{-04}	8×10^{-04}	2×10^{-03}	4×10^{-03}	1×10^{-02}	4×10^{-03}	3×10^{-03}
P-III	Min	6×10^{-01}	3×10^{-01}	8×10^{-02}	1×10^{-01}	1×10^{-01}	1×10^{-01}	5×10^{-02}	6×10^{-02}	1×10^{-01}	2×10^{-01}	1×10^{-01}
	Mean	1×10^{-02}	9×10^{-01}	6×10^{-01}	4×10^{-01}	3×10^{-01}	3×10^{-01}	5×10^{-01}	7×10^{-01}	1×10^{-02}	1×10^{-02}	1×10^{-02}
	SD	4×10^{-01}	4×10^{-01}	4×10^{-01}	4×10^{-01}	3×10^{-01}	1×10^{-01}	3×10^{-01}	2×10^{-01}	2×10^{-02}	4×10^{-01}	4×10^{-01}
	Med	1×10^{-02}	7×10^{-01}	4×10^{-01}	1×10^{-01}	1×10^{-01}	3×10^{-01}	6×10^{-01}	9×10^{-01}	1×10^{-02}	1×10^{-02}	2×10^{-02}
	S.I.R	3×10^{-01}	3×10^{-01}	3×10^{-01}	3×10^{-01}	2×10^{-01}	4×10^{-04}	1×10^{-01}	2×10^{-01}	1×10^{-01}	1×10^{-01}	1×10^{-01}

differential model that lie in good ranges to consider 3, 6 and 10 neurons. It is also noticed that the results based on 10 neurons are more accurate as compared to 3 and 6 number of neurons. The performance indices based on the Fitness (FIT), 'R.MSE', 'EVAF' and 'TIC' are plotted in subfigures 4(a), 4(b) and 4(c) using 3, 6 and 10 neurons. It is clear in

TABLE 4. The statics performances of MWNN-GAIPA for the singular prediction differential model using 10 neurons.

	Mode	$\hat{h}(\tau)$										
		0	0.1	0.2	0.3	0.4	0.5	0.6	0.7	0.8	0.9	1
P-I	Min	3×10^{-08}	3×10^{-06}	1×10^{-06}	2×10^{-06}	8×10^{-07}	5×10^{-06}	4×10^{-05}	9×10^{-05}	6×10^{-05}	5×10^{-04}	1×10^{-03}
	Mean	6×10^{-02}	6×10^{-02}	6×10^{-02}	6×10^{-02}	6×10^{-02}	8×10^{-02}	1×10^{-01}	6×10^{-01}	7×10^{-01}	1×10^{-02}	2×10^{-02}
	SD	1×10^{-01}	1×10^{-01}	1×10^{-01}	1×10^{-01}	1×10^{-01}	1×10^{-01}	3×10^{-01}	8×10^{-01}	1×10^{-02}	1×10^{-02}	2×10^{-02}
	Med	2×10^{-04}	4×10^{-04}	3×10^{-04}	3×10^{-04}	1×10^{-03}	1×10^{-02}	4×10^{-02}	1×10^{-01}	2×10^{-01}	6×10^{-01}	2×10^{-02}
	S.I.R	2×10^{-03}	2×10^{-03}	2×10^{-03}	2×10^{-03}	4×10^{-03}	1×10^{-02}	8×10^{-02}	6×10^{-01}	5×10^{-01}	1×10^{-02}	2×10^{-02}
P-II	Min	9×10^{-06}	6×10^{-06}	7×10^{-06}	1×10^{-06}	3×10^{-06}	9×10^{-06}	1×10^{-05}	4×10^{-05}	2×10^{-05}	9×10^{-06}	3×10^{-06}
	Mean	7×10^{-02}	2×10^{-01}	2×10^{-01}	3×10^{-01}	3×10^{-01}	3×10^{-01}	3×10^{-01}	5×10^{-01}	7×10^{-01}	1×10^{-02}	1×10^{-02}
	SD	2×10^{-01}	4×10^{-01}	5×10^{-01}	5×10^{-01}	5×10^{-01}	5×10^{-01}	5×10^{-01}	7×10^{-01}	1×10^{-02}	2×10^{-02}	4×10^{-02}
	Med	1×10^{-04}	1×10^{-04}	1×10^{-04}	4×10^{-04}	2×10^{-03}	5×10^{-03}	1×10^{-02}	2×10^{-02}	2×10^{-02}	2×10^{-02}	1×10^{-01}
	S.I.R	4×10^{-03}	4×10^{-03}	4×10^{-03}	4×10^{-03}	6×10^{-03}	2×10^{-02}	1×10^{-01}	6×10^{-01}	6×10^{-01}	6×10^{-01}	6×10^{-01}
P-III	Min	1×10^{-08}	2×10^{-06}	1×10^{-06}	7×10^{-06}	1×10^{-06}	7×10^{-06}	6×10^{-05}	3×10^{-05}	2×10^{-05}	5×10^{-06}	3×10^{-04}
	Mean	6×10^{-02}	6×10^{-02}	6×10^{-02}	5×10^{-02}	5×10^{-02}	6×10^{-02}	8×10^{-02}	9×10^{-02}	2×10^{-01}	3×10^{-01}	3×10^{-01}
	SD	1×10^{-01}	1×10^{-01}	1×10^{-01}	1×10^{-01}	1×10^{-01}	1×10^{-01}	2×10^{-01}	2×10^{-01}	6×10^{-01}	9×10^{-01}	6×10^{-01}
	Med	3×10^{-05}	3×10^{-05}	3×10^{-05}	3×10^{-05}	5×10^{-05}	1×10^{-04}	6×10^{-04}	7×10^{-04}	2×10^{-03}	4×10^{-03}	3×10^{-03}
	S.I.R	2×10^{-04}	7×10^{-04}	7×10^{-04}	7×10^{-04}	3×10^{-03}	5×10^{-03}	3×10^{-02}	2×10^{-02}	4×10^{-02}	5×10^{-02}	1×10^{-01}

TABLE 5. Global operator performances for each problem of the singular pantograph model using 3 neurons.

	(G-FIT)		(G-EVAF)		(G-TIC)		(G-RMSE)	
	Min	S.I.R	Min	S.I.R	Min	S.I.R	Min	S.I.R
P-I	1.82E-05	1.06E-01	2.81E-05	1.07E-01	7.69E-07	9.13E-04	2.07E-03	6.56E-01
P-II	5.02E-10	7.00E-04	4.44E-09	1.84E-01	9.29E-09	6.64E-05	2.31E-05	1.79E-01
P-III	1.81E-07	2.77E-01	6.04E-07	2.92E-01	1.09E-07	5.95E-04	2.93E-04	4.43E-01

TABLE 6. Global operator performances for each problem of the singular pantograph model using 6 neurons.

	(G-FIT)		(G-EVAF)		(G-TIC)		(G-RMSE)	
	Min	S.I.R	Min	S.I.R	Min	S.I.R	Min	S.I.R
P-I	3.94E-08	1.98E-01	2.67E-01	1.50E-01	7.25E-05	2.48E-04	2.89E-01	9.42E-01
P-II	1.89E-10	9.68E-06	6.97E-01	1.70E-01	1.35E-04	1.47E-05	5.61E-01	5.82E-02
P-III	2.33E-09	1.14E-01	6.17E-01	2.97E-03	2.26E-04	2.78E-06	9.01E-01	9.60E-03

TABLE 7. Global operator performances for each problem of the singular pantograph model using 10 neurons.

	(G-FIT)		(G-EVAF)		(G-TIC)		(G-RMSE)	
	Min	S.I.R	Min	S.I.R	Min	S.I.R	Min	S.I.R
P-I	1.02E-08	1.16E-03	9.72E-07	1.01E-01	6.74E-08	1.44E-04	3.56E-04	7.78E-01
P-II	4.40E-11	3.64E-04	8.21E-09	4.98E-01	6.93E-09	1.18E-04	3.65E-05	6.24E-01
P-III	3.64E-08	1.79E-04	3.64E-07	6.87E-02	4.32E-08	1.88E-05	2.28E-04	9.92E-02

subfigure 4(a), which is based on 3 neurons that the FIT best values for Problems I, II and III lie in the range of 10^{-04} to 10^{-06}, 10^{-08} to 10^{-10} and 10^{-06} to 10^{-08}, respectively. The R.MSE best values for Problems I, II and III lie around 10^{-02} to 10^{-04}, 10^{-04} to 10^{-06} and 10^{-04} to 10^{-05}. The EVAF best values for Problems I, II and III lie around 10^{-04} to 10^{-06}, 10^{-08} to 10^{-10} and 10^{-06} to 10^{-08}. The TIC best values for Problems I, II and III lie around 10^{-07} to 10^{-08}, 10^{-08} to 10^{-10} and 10^{-07} to 10^{-09}, respectively. The subfigure 4(b), which is based on 6 neurons that the FIT best values for Problems I, II and III lie in the range of 10^{-06} to 10^{-08}, 10^{-09} to 10^{-10} and 10^{-08} to 10^{-09}. The R.MSE best values for Problems I, II and III lie around 10^{-03} to 10^{-04}, 10^{-05} to 10^{-06} and 10^{-04} to 10^{-05}. The EVAF best values for Problems I, II and III lie around 10^{-05} to 10^{-06}, 10^{-09} to 10^{-10} and 10^{-08} to 10^{-09}. The TIC best values for Problems I, II and III lie around 10^{-07} to 10^{-08}, 10^{-08} to 10^{-09} and 10^{-08} to 10^{-09}, respectively. The subfigure 4(c), which is based on 10 neurons that the FIT best values for Problems I, II and III lie in the range of 10^{-07} to 10^{-10}, 10^{-10} to 10^{-11} and 10^{-07} to 10^{-08}. The R.MSE best values for Problems I, II and III lie around 10^{-02} to 10^{-04}, 10^{-04} to 10^{-05} and

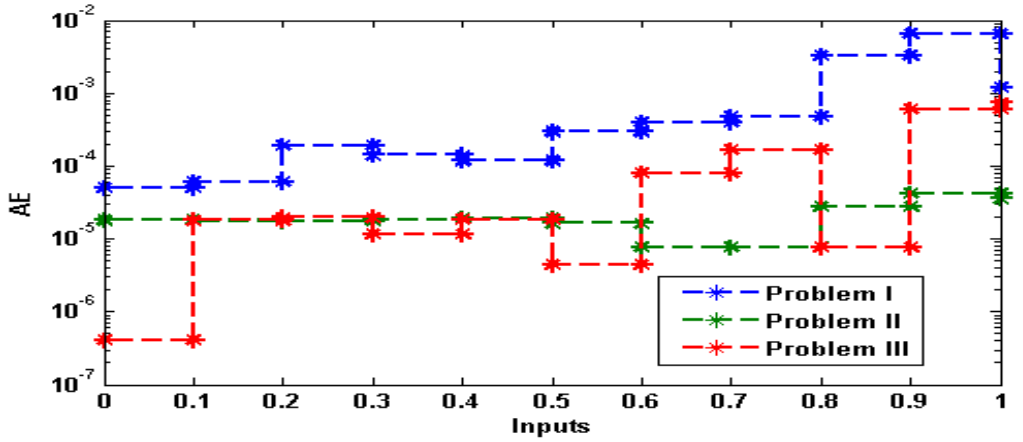

a) AE for all problems of the singular pantograph differential model using 3 neurons

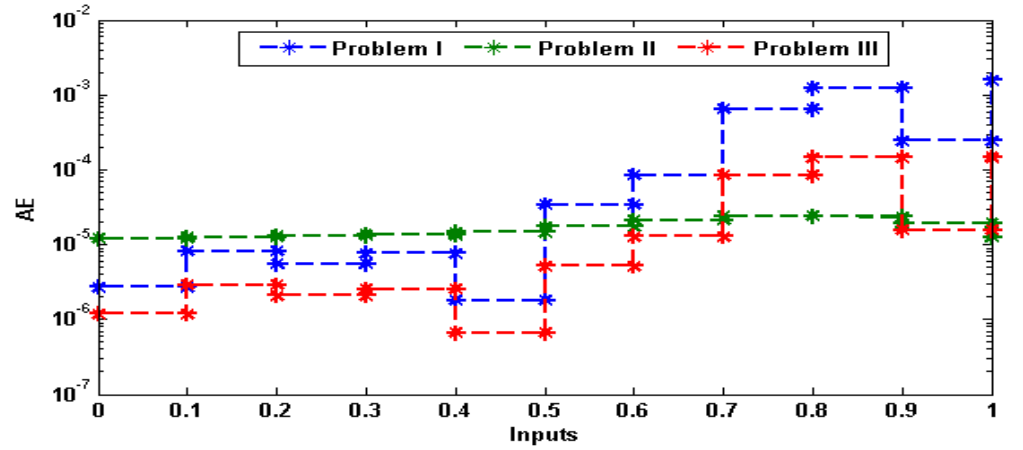

b) AE for all problems of the singular pantograph differential model using 6 neurons

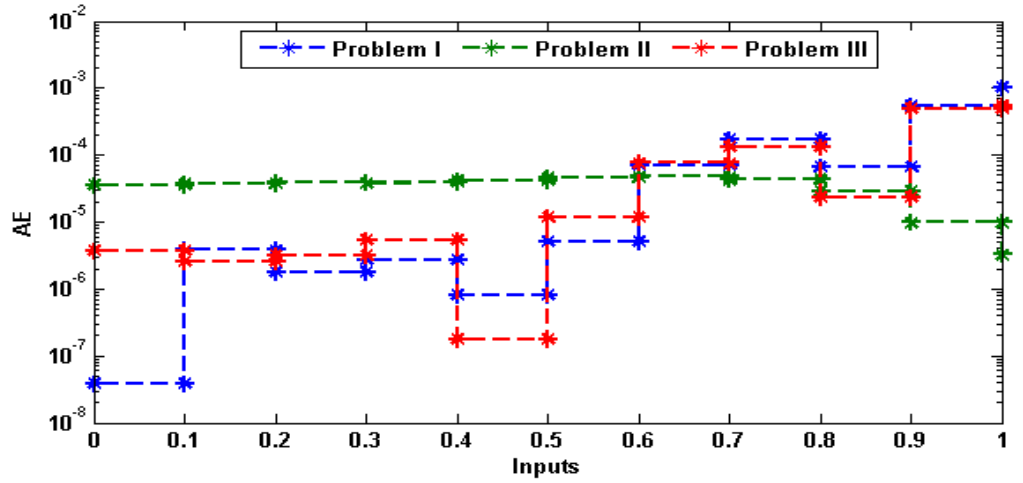

c) AE for all problems of the singular pantograph differential model using 10 neurons

FIGURE 3. AE for each problem of the singular pantograph differential model using 3, 6 and 10 neurons.

10^{-03} to 10^{-04}. The EVAF best values for Problems I, II and III lie around 10^{-06} to 10^{-07}, 10^{-08} to 10^{-09} and 10^{-06} to 10^{-07}. The TIC best values for Problems I, II and III lie around 10^{-06} to 10^{-08}, 10^{-09} to 10^{-10} and 10^{-08} to 10^{-09}, respectively. These attained numerical results confirm the good tendency of performance to solve each problem of the singular pantograph differential model using 3, 6 and 10 neurons.

Statistics graphs of the MWNN-GAIPA for 'FIT', 'R.MSE', 'EVAF' and 'TIC' measures for solving each problem of the singular pantograph differential model are plotted in Figs. 5-8 using 3, 6 and 10 neurons. Fig. 5 shows the

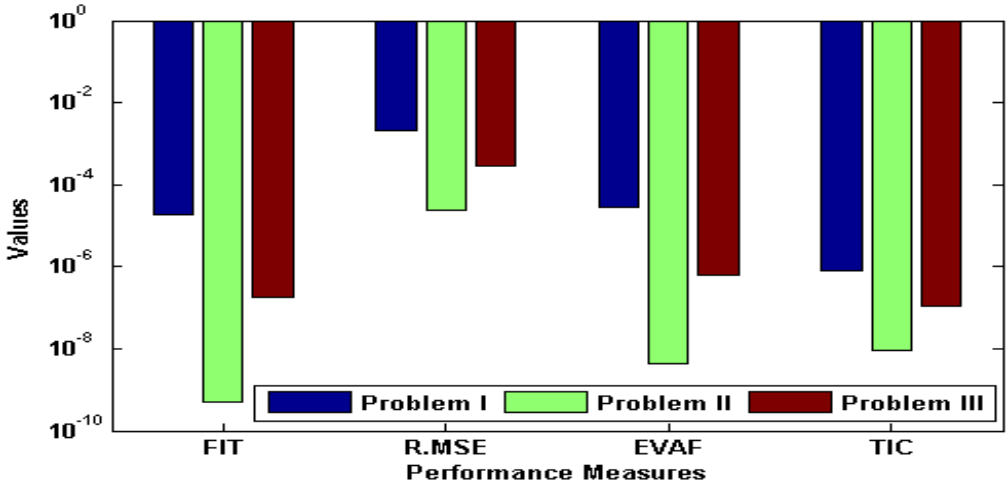

a) Performances for the singular pantograph differential model using 3 neurons

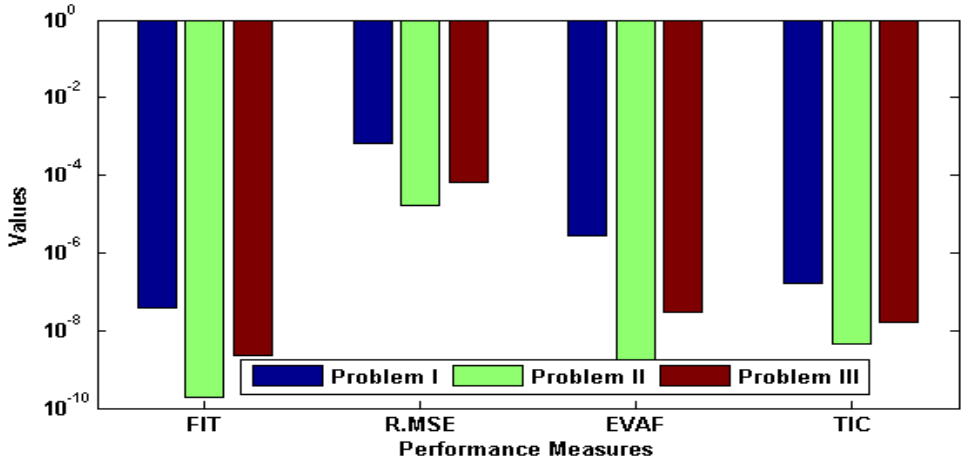

b) Performances for the singular pantograph differential model using 6 neurons

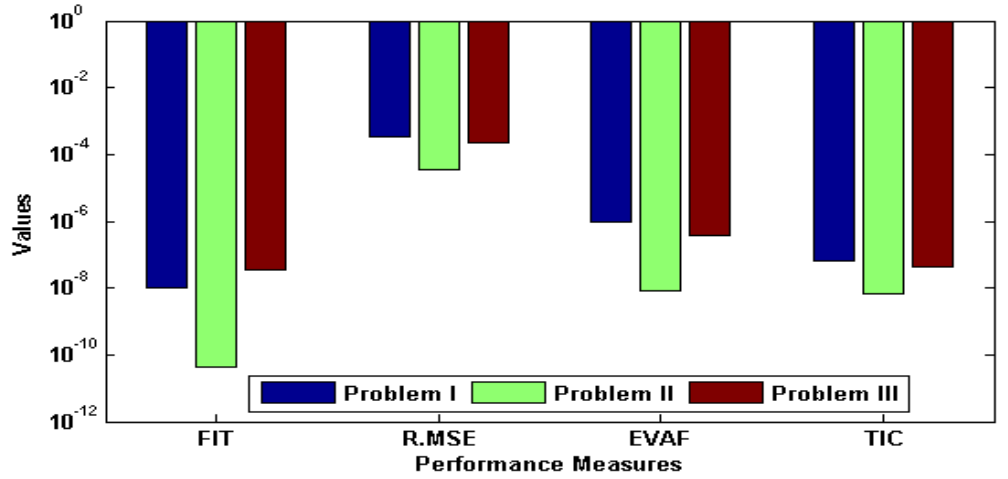

c) Performances for the singular pantograph differential model using 10 neurons

FIGURE 4. Performance values to solve each problem of the singular pantograph differential model using 3, 6 and 10 number of neurons.

performance of FIT for 40 executions to solve the problem of the singular pantograph differential model using 3, 6 and 10 neurons. It is observed that the best trials lie about 10^{-01} to 10^{-03}, 10^{-04} to 10^{-10} and 10^{-02} to 10^{-6} for solving each problem of the singular pantograph differential model using 3 neurons. The FIT performance for 6 neurons is depicted in

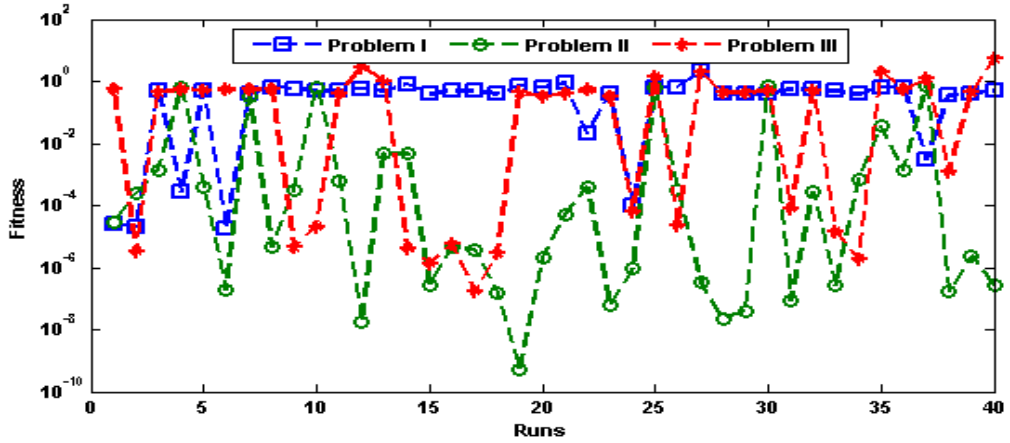

a) FIT convergence plots for each problem of singular pantograph model using 3 neurons

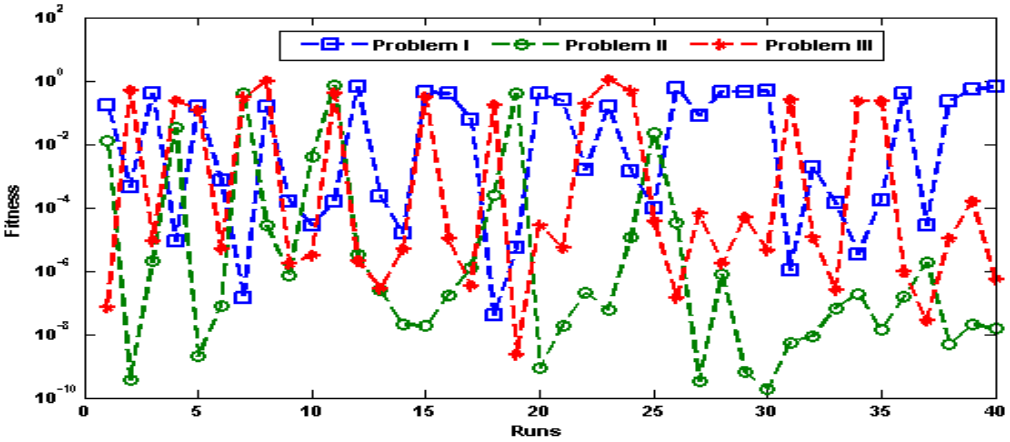

b) FIT convergence plots for each problem of singular pantograph model using 6 neurons

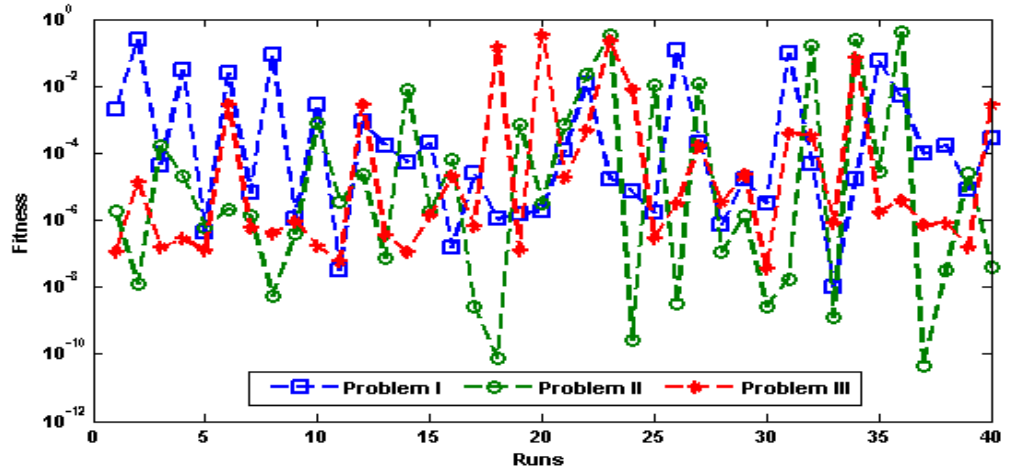

c) FIT convergence plots for each problem of singular pantograph model using 9 neurons

FIGURE 5. Statistical performances through FIT using MWNN-GAIPA for each problem of the singular pantograph differential model taking 3, 6 and 10 neurons.

subfigure 5(b), the best trials lie about 10^{-01} to 10^{-06}, 10^{-04} to 10^{-10} and 10^{-02} to 10^{-08}. While the FIT performance for 10 neurons is depicted in subfigure 5(c), the best trials found around 10^{-02} to 10^{-08}, 10^{-04} to 10^{-12} and 10^{-03} to 10^{-08}. Fig. 6 shows the performance of R.MSE for 40 executions to solve problem of the singular pantograph differential model using 3, 6 and 10 neurons. It is observed that the best trials lie about 10^{-01}, 10^{-02} to 10^{-04} and 10^{-02} to 10^{-06} for solving each problem of the singular pantograph differential model using 3 neurons. The R.MSE performance for 6 neurons is

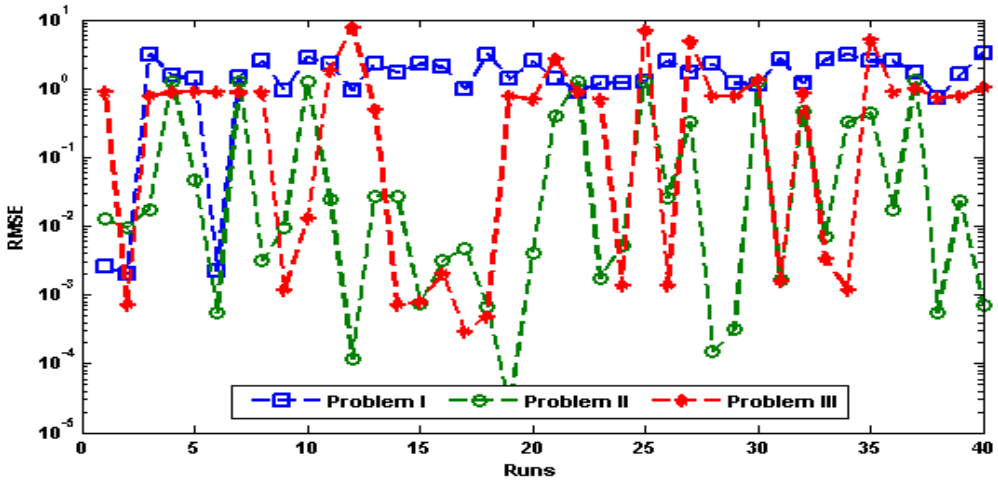

a) RMSE convergence plots for each problem of singular model using 3 neurons

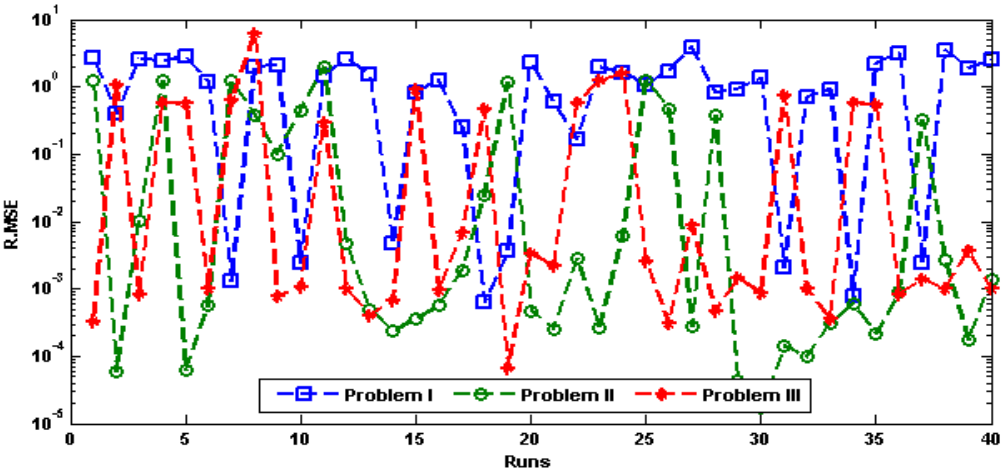

b) RMSE convergence plots for each problem of singular model using 6 neurons

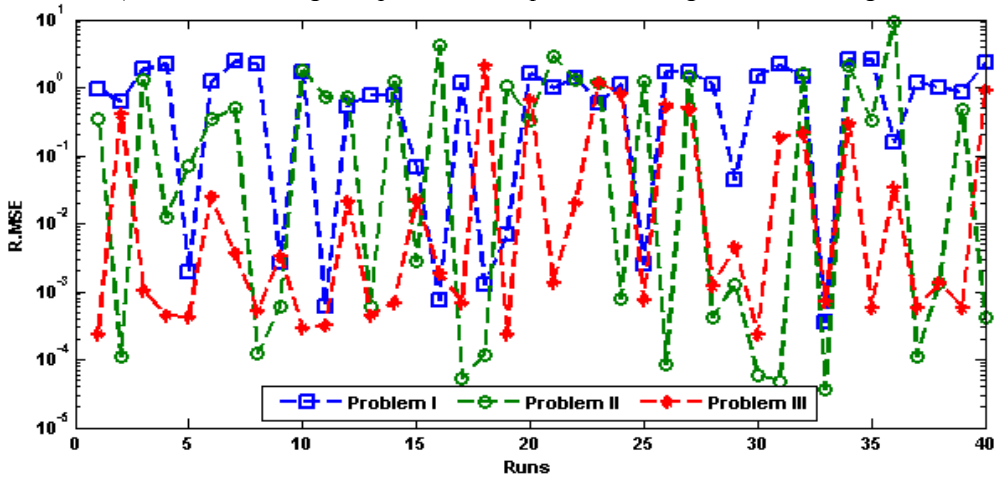

c) RMSE convergence plots for each problem of singular model using 10 neurons

FIGURE 6. Statistical performances through RMSE using MWNN-GAIPA for each problem of the singular pantograph differential model taking 3, 6 and 10 neurons.

depicted in subfigure 6(b), the best trials lie about 10^{-01} to 10^{-03}, 10^{-02} to 10^{-05} and 10^{-01} to 10^{-04}. While the R.MSE performance for 10 neurons is depicted in subfigure 6(c), the best trials found around 10^{-01} to 10^{-04}, 10^{-01} to 10^{-05} and 10^{-01} to 10^{-04}. Fig. 7 shows the performance of EVAF for 40 executions to solve problem of the singular pantograph

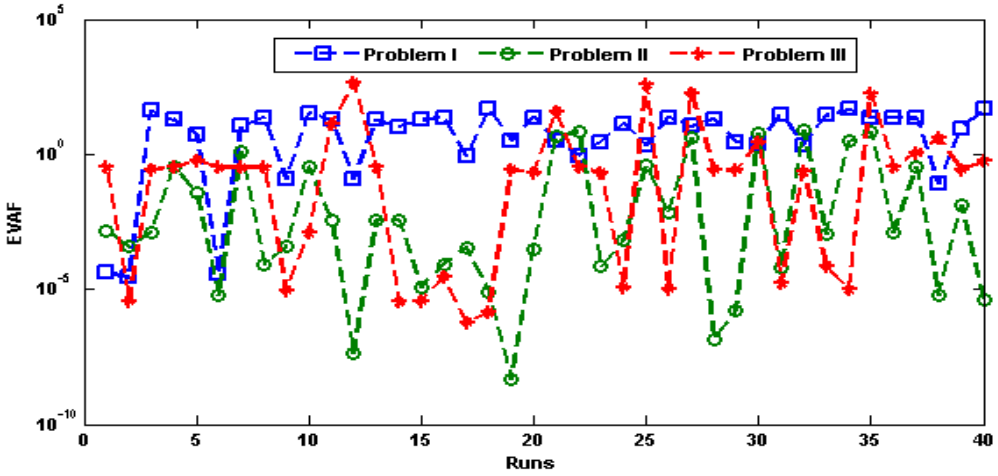

a) EVAF convergence plots for each problem of singular model using 3 neurons

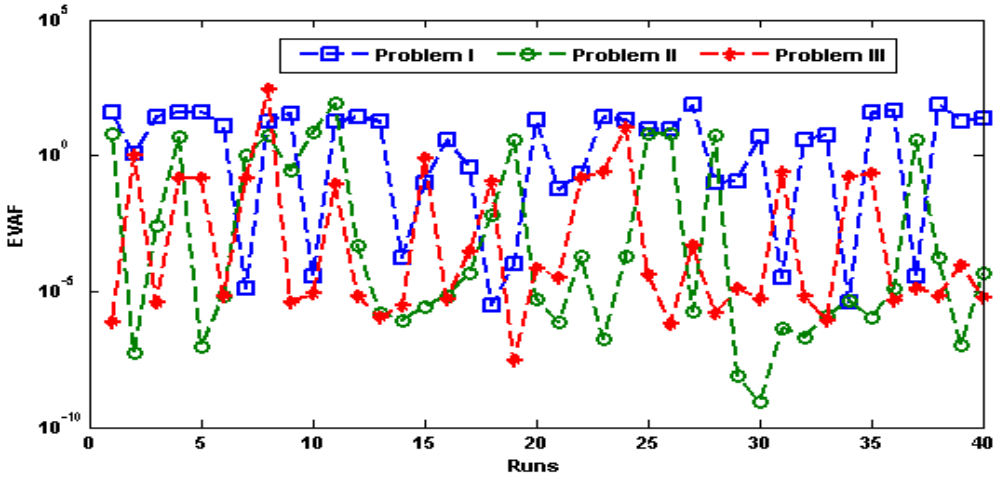

b) EVAF convergence plots for each problem of singular model using 6 neurons

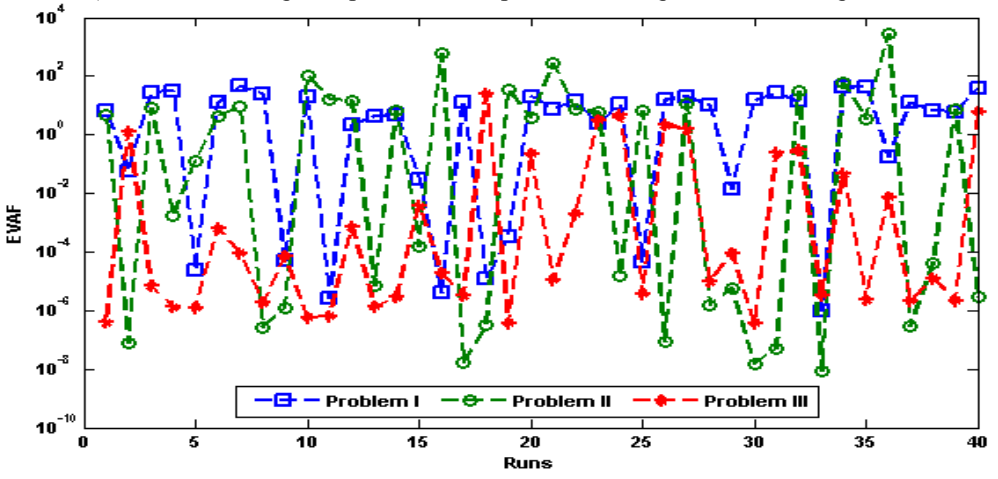

c) RMSE convergence plots for each problem of singular model using 10 neurons

FIGURE 7. Statistical performances through EVAF using MWNN-GAIPA for each problem of the singular pantograph differential model taking 3, 6 and 10 neurons.

differential model using 3, 6 and 10 neurons. It is observed that the best trials lie about 10^{-01} to 10^{-02}, 10^{-02} to 10^{-07} and 10^{-02} to 10^{-05} for solving each problem of the singular pantograph differential model using 3 neurons. The EVAF performance for 6 neurons is depicted in subfigure 7(b), the best trials lie about 10^{-01} to 10^{-05}, 10^{-02} to 10^{-08} and

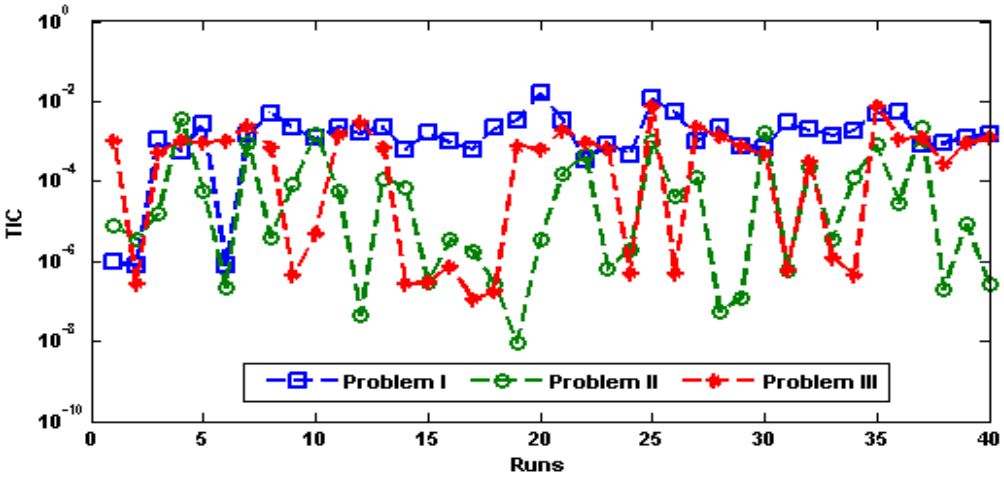

a) convergence plots for each problem of singular model using 3 neurons

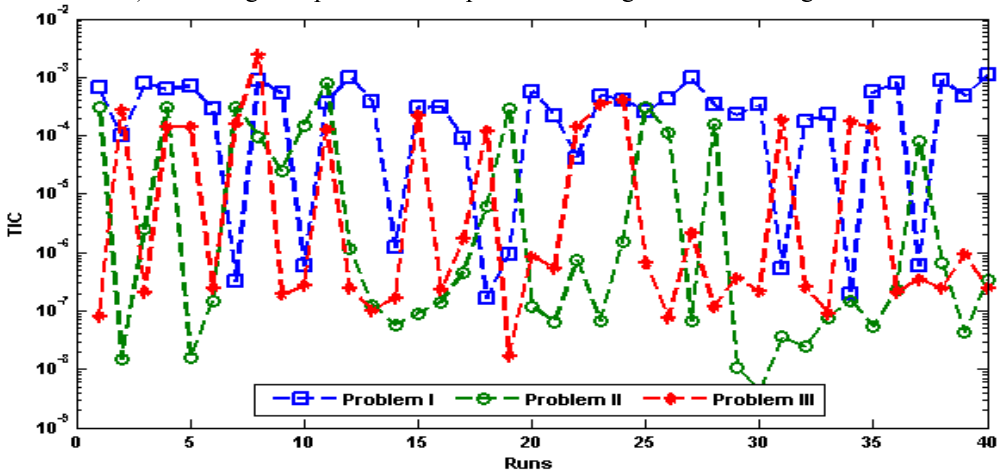

b) convergence plots for each problem of singular model using 3 neurons

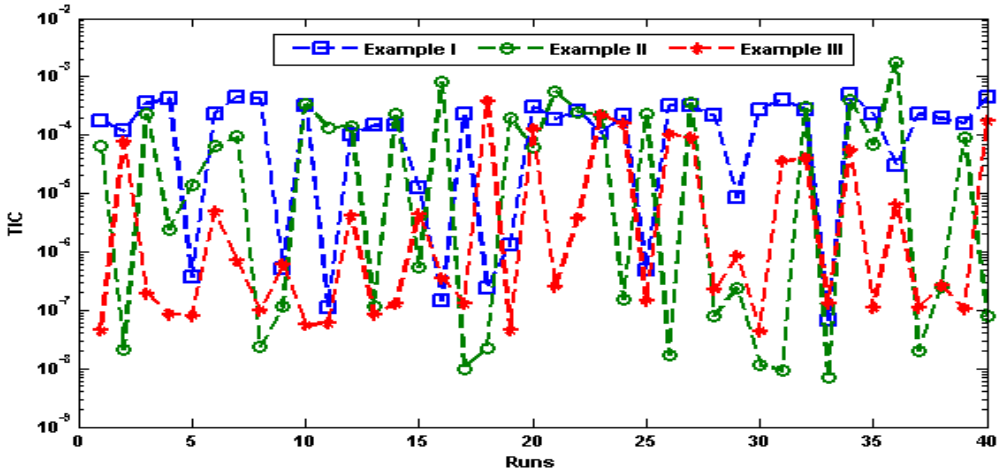

c) convergence plots for each problem of singular model using 3 neurons

FIGURE 8. Statistical performances through TIC using MWNN-GAIPA for each problem of the singular pantograph differential model taking 3, 6 and 10 neurons.

10^{-02} to 10^{-06}. While the EVAF performance for 10 neurons is depicted in subfigure 7(c), the best trials found around 10^{-01} to 10^{-04}, 10^{-02} to 10^{-08} and 10^{-02} to 10^{-06}. Fig. 8 shows the performance of TIC for 40 executions to solve problem of the singular pantograph differential model using 3, 6 and 10 neurons. It is observed that the best trials lie

about 10^{-02} to 10^{-05}, 10^{-03} to 10^{-09} and 10^{-03} to 10^{-08} for solving each problem of the singular pantograph differential model using 3 neurons. The TIC performance for 6 neurons is depicted in subfigure 8(b), the best trials lie about 10^{-03} to 10^{-07}, 10^{-04} to 10^{-09} and 10^{-04} to 10^{-08}. While the EVAF performance for 10 neurons is depicted in subfigure 8(c), the best trials found around 10^{-04} to 10^{-08}, 10^{-05} to 10^{-09} and 10^{-04} to 10^{-08}. One can easily understand that by taking three numbers of neurons the scheme performance is getting better by enlarging the number of neurons.

The global operators via MWNN-GAIPA to solve each problem of the singular pantograph differential model for 40 trials using 3, 6 and 10 neurons are given in Table 5-7. The statistical measures of the global FIT, EVAF, TIC and R.MSE operators based on Min and S.I.R gages for 3, 6 and 10 neurons have been tabulated. The calculated optimum smaller values based on these statistical measures authenticate the accuracy as well as precision of MWNN-GAIPA scheme. While with increase in number of neuron the computational time complexity of the proposed integrated heuristic MWNN-GAIPA increases i.e., 15 ± 5 for 3 neurons models, 34 ± 7 for 6 neuron models and 71 ± 12 for 10 neuron models. One can observe that by taking a larger number of neurons the performance of the scheme is better as compared to lesser number of neurons but at the cost of relatively more computations.

V. CONCLUSION

The present study is related to design a Morlet wavelet neural network for solving the singular pantograph differential model. The singular pantograph differential model is one of the important kind of functional differential model. The hybridization of the global and local search operators, i.e., GA-IPA is used in the optimization process. To observe the correctness of the MWNN-GAIPA, the numerical results have been compared with the exact solutions for each problem of the singular pantograph differential model. In order to check the accuracy of the designed MWNN-GAIPA scheme, the neuron analysis based on 3, 6 and 10 neurons have been provided for 40 trials using different statistical measures. It is observed that the performance of the scheme for 3 neurons is better, but performance is calculated slightly better for 6 and 10 neurons. It is also observed that the matching of the obtained and exact results has been performed for all the neurons. Moreover, statistical performances using the operators Min, SD, Med, mean and S.I.R authenticate the trustworthiness and accurateness of the proposed MWNN-GAIPA scheme. The global EVAF, TIC and R.MSE further validate the performance of the designed MWNN-GAIPA scheme to solve each problem of the singular pantograph differential model. There are various traditional schemes that do not work to solve the singular models. The singular pantograph model becomes stiffer and not easy to handle using the conventional schemes. So MWNN is the best choice to solve such complicated models using the global and local search terminologies GAIPA. In future, MWNN-GAIPA can be implemented to solve the fluid dynamic nonlinear systems, biological nonlinear systems, singular higher order differential systems, fractional processing, direction of arrival estimation, power and eneggy systems [53]–[62].

ACKNOWLEDGMENT

The authors would like to thank Prof. D. P. Kothari (IEEE Fellow and IEEE Access journal, Senior Editor) for his valuable comments and suggestions on improving the article.

REFERENCES

[1] J. R. Ockendon and A. B. Tayler, "The dynamics of a current collection system for an electric locomotive," *Proc. Roy. Soc. London. A. Math. Phys. Sci.*, vol. 322, no. 1551, 1971, pp. 447–468. Accessed: Feb. 8, 2021, doi: 10.1098/rspa.1971.0078.

[2] V. Spiridonov, "Universal superpositions of coherent states and self-similar potentials," *Phys. Rev. A, Gen. Phys.*, vol. 52, no. 3, p. 1909, 1995.

[3] G. C. Wake, S. Cooper, H. K. Kim, and B. Van-Brunt, "Functional differential equations for cell-growth models with dispersion," *Commun. Appl. Anal.*, vol. 4, no. 4, pp. 561–574, 2000.

[4] A. S. C. Sinha, "Stabilisation of time-varying infinite delay control systems," *IEE Proc. D (Control Theory Appl.)*, vol. 140, no. 1, pp. 60–63, 1993.

[5] I. Khan, M. A. Z. Raja, M. Shoaib, P. Kumam, H. Alrabaiah, Z. Shah, and S. Islam, "Design of neural network with Levenberg-Marquardt and Bayesian regularization backpropagation for solving pantograph delay differential equations," *IEEE Access*, vol. 8, pp. 137918–137933, 2020.

[6] S. S. Ezz-Eldien, Y. Wang, M. A. Abdelkawy, M. A. Zaky, A. A. Aldraiweesh, and J. T. Machado, "Chebyshev spectral methods for multi-order fractional neutral pantograph equations," *Nonlinear Dyn.*, vol. 100, no. 4, pp. 3785–3797, Jun. 2020.

[7] S. S. Ezz-Eldien, "On solving systems of multi-pantograph equations via spectral tau method," *Appl. Math. Comput.*, vol. 321, pp. 63–73, Mar. 2018.

[8] N. R. Anakira, A. Jameel, A.-K. Alomari, A. Saaban, M. Almahameed, and I. Hashim, "Approximate solutions of multi-pantograph type delay differential equations using multistage optimal homotopy asymptotic method," *J. Math. Fundam. Sci.*, vol. 50, no. 3, pp. 221–232, 2018.

[9] A. Isah and C. Phang, "A collocation method based on Genocchi operational matrix for solving Emden-Fowler equations," *J. Phys., Conf. Ser.*, vol. 1489, no. 1, 2020, Art. no. 012022.

[10] S. Yousefi, M. Noei-Khorshidi, and A. Lotfi, "Convergence analysis of least squares-Epsilon-Ritz algorithm for solving a general class of pantograph equations," *Kragujevac J. Math.*, vol. 42, no. 3, pp. 431–439, 2018.

[11] S. Yüzbasi and N. Ismailov, "A Taylor operation method for solutions of generalized pantograph type delay differential equations," *Turkish J. Math.*, vol. 42, no. 2, pp. 395–406, Mar. 2018.

[12] B. N. Saray and J. Manafian, "Sparse representation of delay differential equation of pantograph type using multi-wavelets Galerkin method," *Eng. Comput.*, vol. 35, no. 2, pp. 887–903, Apr. 2018, doi: 10.1108/EC-08-2017-0299.

[13] M. A. Z. Raja, "Numerical treatment for boundary value problems of pantograph functional differential equation using computational intelligence algorithms," *Appl. Soft Comput.*, vol. 24, pp. 806–821, Nov. 2014.

[14] J. Zhao, Y. Cao, and Y. Xu, "Sinc numerical solution for pantograph Volterra delay-integro-differential equation," *Int. J. Comput. Math.*, vol. 94, no. 5, pp. 853–865, May 2017.

[15] M. S. M. Bahgat, "Approximate analytical solution of the linear and nonlinear multi-pantograph delay differential equations," *Phys. Scripta*, vol. 95, no. 5, May 2020, Art. no. 055219.

[16] M. A. Abdelkawy, Z. Sabir, J. L. G. Guirao, and T. Saeed, "Numerical investigations of a new singular second-order nonlinear coupled functional Lane–Emden model," *Open Phys.*, vol. 18, no. 1, pp. 770–778, Nov. 2020.

[17] R. Katani, "Multistep block method for linear and nonlinear pantograph type delay differential equations with neutral term," *Int. J. Appl. Comput. Math.*, vol. 3, no. 1, pp. 1347–1359, Dec. 2017.

[18] H. Ansari and P. Mokhtary, "Computational Legendre Tau method for Volterra Hammerstein pantograph integral equations," *Bull. Iranian Math. Soc.*, vol. 45, no. 2, pp. 475–493, Apr. 2019.

[19] Y. Cong, W. Zhan, and Q. Guo, "The partially truncated Euler–Maruyama method for highly nonlinear stochastic delay differential equations with Markovian switching," *Int. J. Comput. Methods*, vol. 17, no. 6, Aug. 2020, Art. no. 1950014.
[20] T. Luo, Z. Xin, and H. Zeng, "Nonlinear asymptotic stability of the Lane–Emden solutions for the viscous gaseous star problem with degenerate density dependent viscosities," *Commun. Math. Phys.*, vol. 347, no. 3, pp. 657–702, Nov. 2016.
[21] K. Boubaker and R. A. Van Gorder, "Application of the BPES to Lane–Emden equations governing polytropic and isothermal gas spheres," *New Astron.*, vol. 17, no. 6, pp. 565–569, Aug. 2012.
[22] R. Rach, J.-S. Duan, and A.-M. Wazwaz, "Solving coupled Lane–Emden boundary value problems in catalytic diffusion reactions by the adomian decomposition method," *J. Math. Chem.*, vol. 52, no. 1, pp. 255–267, Jan. 2014.
[23] Z. Sabir, M. A. Z. Raja, M. Umar, and M. Shoaib, "Neuro-swarm intelligent computing to solve the second-order singular functional differential model," *Eur. Phys. J. Plus*, vol. 135, no. 6, pp. 1–19, Jun. 2020.
[24] I. Ahmad, M. A. Z. Raja, M. Bilal, and F. Ashraf, "Bio-inspired computational heuristics to study Lane–Emden systems arising in astrophysics model," *SpringerPlus*, vol. 5, no. 1, pp. 1–23, Dec. 2016.
[25] Z. Sabir, M. A. Raja, A. Arbi, G. C. Altamirano, and J. Cao, "Neuro-swarms intelligent computing using Gudermannian kernel for solving a class of second order Lane-Emden singular nonlinear model," *AIMS Math.*, vol. 6, no. 3, pp. 2468–2485, 2021.
[26] Z. Sabir, D. Baleanu, M. A. Z. Raja, and J. L. G. Guirao, "Design of neuro-swarming heuristic solver for multi-pantograph singular delay differential equation," *Fractals*, vol. 29, no. 5, pp. 2140022-1–2140022-16, 2021, doi: 10.1142/S0218348X21400223.
[27] M. Umar, Z. Sabir, M. A. Z. Raja, and Y. G. Sánchez, "A stochastic numerical computing heuristic of SIR nonlinear model based on dengue fever," *Results Phys.*, vol. 19, Dec. 2020, Art. no. 103585.
[28] M. Umar, Z. Sabir, and M. A. Z. Raja, "Intelligent computing for numerical treatment of nonlinear prey–predator models," *Appl. Soft Comput.*, vol. 80, pp. 506–524, Jul. 2019.
[29] M. Umar, Z. Sabir, M. A. Z. Raja, F. Amin, T. Saeed, and Y. Guerrero-Sanchez, "Integrated neuro-swarm heuristic with interior-point for nonlinear SITR model for dynamics of novel COVID-19," *Alexandria Eng. J.*, vol. 60, no. 3, pp. 2811–2824, Jun. 2021, doi: 10.1016/j.aej.2021.01.043.
[30] H. Ilyas, I. Ahmad, M. A. Z. Raja, and M. Shoaib, "A novel design of Gaussian WaveNets for rotational hybrid nanofluidic flow over a stretching sheet involving thermal radiation," *Int. Commun. Heat Mass Transf.*, vol. 123, Apr. 2021, Art. no. 105196.
[31] M. Umar, Z. Sabir, F. Amin, J. L. G. Guirao, and M. A. Z. Raja, "Stochastic numerical technique for solving HIV infection model of CD4+T cells," *Eur. Phys. J. Plus*, vol. 135, no. 5, p. 403, May 2020.
[32] Z. Sabir, M. A. Z. Raja, J. L. G. Guirao, and M. Shoaib, "A neuro-swarming intelligence-based computing for second order singular periodic non-linear boundary value problems," *Frontiers Phys.*, vol. 8, p. 224, Aug. 2020.
[33] A. H. Bukhari, M. A. Z. Raja, M. Sulaiman, S. Islam, M. Shoaib, and P. Kumam, "Fractional neuro-sequential ARFIMA-LSTM for financial market forecasting," *IEEE Access*, vol. 8, pp. 71326–71338, 2020.
[34] M. A. Z. Raja, J. Mehmood, Z. Sabir, A. K. Nasab, and M. A. Manzar, "Numerical solution of doubly singular nonlinear systems using neural networks-based integrated intelligent computing," *Neural Comput. Appl.*, vol. 31, no. 3, pp. 793–812, Mar. 2019.
[35] Z. Sabir, M. Umar, J. L. G. Guirao, M. Shoaib, and M. A. Z. Raja, "Integrated intelligent computing paradigm for nonlinear multi-singular third-order Emden–Fowler equation," *Neural Comput. Appl.*, vol. 33, no. 8, pp. 3417–3436, Apr. 2021, doi: 10.1007/s00521-020-05187-w.
[36] M. Umar, Z. Sabir, M. A. Z. Raja, M. Shoaib, M. Gupta, and Y. G. Sánchez, "A stochastic intelligent computing with neuro-evolution heuristics for nonlinear SITR system of novel COVID-19 dynamics," *Symmetry*, vol. 12, no. 10, p. 1628, Oct. 2020. Accessed: Jan. 5, 2021, doi: 10.3390/sym12101628.
[37] M. A. Z. Raja, M. Umar, Z. Sabir, J. A. Khan, and D. Baleanu, "A new stochastic computing paradigm for the dynamics of nonlinear singular heat conduction model of the human head," *Eur. Phys. J. Plus*, vol. 133, no. 9, p. 364, Sep. 2018.
[38] Z. Sabir, H. A. Wahab, M. Umar, M. G. Sakar, and M. A. Z. Raja, "Novel design of Morlet wavelet neural network for solving second order Lane–Emden equation," *Math. Comput. Simul.*, vol. 172, pp. 1–14, Jun. 2020.
[39] Z. Sabir, M. A. Z. Raja, J. L. G. Guirao, and M. Shoaib, "A novel design of fractional Meyer wavelet neural networks with application to the nonlinear singular fractional Lane-Emden systems," *Alexandria Eng. J.*, vol. 60, no. 2, pp. 2641–2659, Apr. 2021.
[40] Z. Sabir, M. A. Z. Raja, and D. Baleanu, "Fractional mayer neuro-swarm heuristic solver for multi-fractional order doubly singular model based on lane-emden equation," *Fractals*, vol. 29, no. 5, pp. 2140017-1–2140017-15, 2021, doi: 10.1142/S0218348X2140017X.
[41] Z. Sabir, M. A. Z. Raja, M. Shoaib, and J. F. G. Aguilar, "FMNEICS: Fractional Meyer neuro-evolution-based intelligent computing solver for doubly singular multi-fractional order Lane–Emden system," *Comput. Appl. Math.*, vol. 39, no. 4, pp. 1–18, Dec. 2020.
[42] G. T. Reddy, M. P. K. Reddy, K. Lakshmanna, D. S. Rajput, R. Kaluri, and G. Srivastava, "Hybrid genetic algorithm and a fuzzy logic classifier for heart disease diagnosis," *Evol. Intell.*, vol. 13, no. 2, pp. 185–196, Jun. 2020.
[43] A. Mehmood, A. Zameer, S. H. Ling, A. U. Rehman, and M. A. Z. Raja, "Integrated computational intelligent paradigm for nonlinear electric circuit models using neural networks, genetic algorithms and sequential quadratic programming," *Neural Comput. Appl.*, vol. 32, no. 14, pp. 10337–10357, Jul. 2020.
[44] Z. Sabir, S. Saoud, M. A. Z. Raja, H. A. Wahab, and A. Arbi, "Heuristic computing technique for numerical solutions of nonlinear fourth order Emden–Fowler equation," *Math. Comput. Simul.*, vol. 178, pp. 534–548, Dec. 2020.
[45] I. Ahmad, S. Ahmad, M. Awais, S. U. I. Ahmad, and M. A. Z. Raja, "Neuro-evolutionary computing paradigm for Painlevé equation-II in nonlinear optics," *Eur. Phys. J. Plus*, vol. 133, no. 5, p. 184, May 2018.
[46] D. J. Armaghani, M. Hasanipanah, A. Mahdiyar, M. Z. A. Majid, H. B. Amnieh, and M. M. D. Tahir, "Airblast prediction through a hybrid genetic algorithm-ANN model," *Neural Comput. Appl.*, vol. 29, no. 9, pp. 619–629, May 2018.
[47] Z. Sabir, M. A. Manzar, M. A. Z. Raja, M. Sheraz, and A. M. Wazwaz, "Neuro-heuristics for nonlinear singular Thomas-Fermi systems," *Appl. Soft Comput.*, vol. 65, pp. 152–169, Apr. 2018.
[48] Y. Jiang, P. Wu, J. Zeng, Y. Zhang, Y. Zhang, and S. Wang, "Multi-parameter and multi-objective optimisation of articulated monorail vehicle system dynamics using genetic algorithm," *Vehicle Syst. Dyn.*, vol. 58, no. 1, pp. 74–91, Jan. 2020.
[49] C. Bertocchi, E. Chouzenoux, M.-C. Corbineau, J.-C. Pesquet, and M. Prato, "Deep unfolding of a proximal interior point method for image restoration," *Inverse Problems*, vol. 36, no. 3, Mar. 2020, Art. no. 034005.
[50] S. Pesteh, H. Moayyed, and V. Miranda, "Favorable properties of interior point method and generalized correntropy in power system state estimation," *Electr. Power Syst. Res.*, vol. 178, Jan. 2020, Art. no. 106035.
[51] S. E. Wright and S. Lim, "Solving nested-constraint resource allocation problems with an interior point method," *Oper. Res. Lett.*, vol. 48, no. 3, pp. 297–303, May 2020.
[52] S. Garreis, T. M. Surowiec, and M. Ulbrich, "An interior-point approach for solving risk-averse PDE-constrained optimization problems with coherent risk measures," *SIAM J. Optim.*, vol. 31, no. 1, pp. 1–29, Jan. 2021.
[53] M. Shoaib, M. A. Z. Raja, M. T. Sabir, A. H. Bukhari, H. Alrabaiah, Z. Shah, P. Kumam, and S. Islam, "A stochastic numerical analysis based on hybrid NAR-RBFs networks nonlinear SITR model for novel COVID-19 dynamics," *Comput. Methods Programs Biomed.*, vol. 202, Apr. 2021, Art. no. 105973.
[54] N. Ahmed, H. Wang, M. A. Z. Raja, W. Ali, F. Zaman, W. U. Khan, and Y. He, "Performance analysis of efficient computing techniques for direction of arrival estimation of underwater multi targets," *IEEE Access*, vol. 9, pp. 33284–33298, 2021.
[55] Z. Sabir, M. G. Sakar, M. Yeskindirova, and O. Saldir, "Numerical investigations to design a novel model based on the fifth order system of Emden–Fowler equations," *Theor. Appl. Mech. Lett.*, vol. 10, no. 5, pp. 333–342, Jul. 2020.
[56] M. M. Almalki, E. S. Alaidarous, D. A. Maturi, M. A. Z. Raja, and M. Shoaib, "A Levenberg–Marquardt backpropagation neural network for the numerical treatment of squeezing flow with heat transfer model," *IEEE Access*, vol. 8, pp. 227340–227348, 2020.
[57] M. Umar, Z. Sabir, A. Imran, A. Wahab, M. Shoaib, and M. Raja, "The 3-D flow of casson nanofluid over a stretched sheet with chemical reactions, velocity slip, thermal radiation and Brownian motion," *Thermal Sci.*, vol. 24, no. 5, pp. 2929–2939, 2020. Accessed: Jan. 5, 2021. [Online]. Available: http://www.doiserbia.nb.rs/img/doi/0354-9836/2020/0354-98361900339U.pdf

[58] H. A. Mirza, M. A. Z. Raja, N. I. Chaudhary, I. M. Qureshi, and A. N. Malik, "A robust multi sample compressive sensing technique for DOA estimation using sparse antenna array," *IEEE Access*, vol. 8, pp. 140848–140861, 2020.
[59] Y. Muhammad, R. Khan, M. A. Z. Raja, F. Ullah, N. I. Chaudhary, and Y. He, "Design of fractional swarm intelligent computing with entropy evolution for optimal power flow problems," *IEEE Access*, vol. 8, pp. 111401–111419, 2020.
[60] N. H. Khan, Y. Wang, D. Tian, M. A. Z. Raja, R. Jamal, and Y. Muhammad, "Design of fractional particle swarm optimization gravitational search algorithm for optimal reactive power dispatch problems," *IEEE Access*, vol. 8, pp. 146785–146806, 2020.
[61] R. Jamal, B. Men, N. H. Khan, M. A. Z. Raja, and Y. Muhammad, "Application of Shannon entropy implementation into a novel fractional particle swarm optimization gravitational search algorithm (FPSOGSA) for optimal reactive power dispatch problem," *IEEE Access*, vol. 9, pp. 2715–2733, 2020.

KASHIF NISAR (Senior Member, IEEE) received the Ph.D. degree from the Universiti Teknologi PETRONAS, Malaysia. He held postdoctoral position at the Auckland University of Technology, Auckland, New Zealand. Through his major in computer network and information technology, he has obtained solid training in research and development, writing funding proposal, journal publication, and as a consultant. He has worked as a Guest Professor with the Fernuniversität Hagen, Germany, in 2014, fully funded by DAAD. He holds a number of visiting professor positions in well-known universities such as McMaster University, Hamilton, ON, Canada, University of Auckland, New Zealand, Hanyang University, South Korea, and Waseda University, Tokyo, Japan. He is currently working as an Associate Professor with the Faculty of Computing and Informatics, University Malaysia Sabah, Kota Kinabalu, Malaysia. He has been published more than 160 research articles in many high impact journals and well reputed international conferences proceeding in the area of computer network. His research interests include future Internet, information centric networks, content-centric networking, named data networking, software-defined networking, the Internet of Things, the Internet of Everything, the Industrial Internet of Things, fourth industrial revolution (IR 4.0), quantum networks, artificial neural networks, information security and privacy network/cyber security, digital forensics, applied cryptography, vehicular clouds, cloud and edge computing, and blockchain. He is working on future networks, the IoT security and API security and he is also working closely with industry. He is a member of many professional organizations from academia and industry, including the Founding Vice-Chair of the IEEE Sabah Subsection, Malaysia, a member of ACM, ACM-SIGMOBILE, ISOC, Engineers Australia, IAENG, Park Laboratory, and a Fellow of APAN and ITU. He is serving as an Editorial Board Member for various journals, including *Computer Communication* Elsevier, *Internet Technology Letters* (Wiley), and serves as a reviewer for most of the IEEE TRANSACTIONS, Springer, and Elsevier journals. He also serves as a Technical Program Committee Member of various conferences, such as IEEE GLOBECOM, IEEE R10 TENCOM, IEEE TrustCom, IEEE ICC, IEEE VTC, IEEE VNC, IEEE ICCVE, and ICCCN. He is also serving as a guest editor for more than a dozen special issues in journals and magazines, such as IEEE, Elsevier, Springer, and Wiley.

ZULQURNAIN SABIR received the M.Sc. degree in mathematics from Punjab University, Lahore, Pakistan, and the M.Phil. degree in mathematics from Preston University Kohat, Islamabad Campus, Pakistan. He is currently pursuing the Ph.D. degree in mathematics with Hazara University, Mansehra, Pakistan. He is famous to solve singular models, functional models, fractional models, biological models and fluid models. He is a pioneer to design and solve second order pantograph Emden-Fowler model, prediction differential model, nonlinear fifth order Emden-Fowler model, nervous stomach model, and nonlinear multi-singular SITR model-based on coronavirus (COVID 19). He has published more than 50 articles in reported international WoS journals with Impact Factors. His research interests include mathematical modeling, unsupervised neural networks, supervised neural networks, artificial intelligence, and implementation of computational techniques-based on traditional as well as heuristic methodology.

MUHAMMAD ASIF ZAHOOR RAJA received the M.Sc. degree in mathematics from Forman Christen College, Lahore, Pakistan, in 1996, the M.Sc. degree in nuclear engineering from Quaid-e-Azam, University, Islamabad, Pakistan, in 1999, and the Ph.D. degree in electronic engineering from International Islamic University, Islamabad, in 2011. From 1999 to 2012, he was involved in research and development assignment of Engineering and Scientific Commission of Pakistan. He is currently working as an Assistant Professor with the Department of Electrical Engineering, COMSATS Institute of Information Technology, Attock Campus, Attock, Pakistan, and associated with the Future Technology Research Center, National Yunlin University of Science and Technology, Yunlin, Taiwan, R.O.C., for the research work. He has developed the Fractional least mean square algorithm and computational platform is formulated for the first time for solving fractional differential equation using artificial intelligence techniques during his Ph.D. studies. He has been the author of more than 200 publications, out of which more than 199 are reputed journal publications with impact factor $750+. He acts as a resource person and gives invited talks on many workshops and conferences held at the national level. His research interests include solving linear and nonlinear differential equation of arbitrary order, active noise control systems, fractional adaptive signal processing, nonlinear system identification, direction of arrival estimation, and bioinformatics problems.

AG. ASRI AG. IBRAHIM (Member, IEEE) received the bachelor's and master's degrees in computer science from the University of Malaya, Malaysia, and the Doctor of Philosophy degree in electronics from The University of York, U.K. He is currently working as the Director of JTMK, University Malaysia Sabah, Labuan Campus and Kota Kinabalu Campus, Sabah, Malaysia. He has been a member of the university senate for more than ten years. He is also the Chairman of the Malaysia Association of Kansei Engineering (MAKE) for the Sabah Region. His research interests include sonification, Kansei engineering, and human–computer interaction.

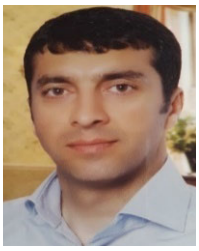

FEVZI ERDOGAN received the M.S. and Ph.D. degrees in mathematics from Yuzuzncu Yil University, Van, Turkey. He is involved in research and work with the Department of Mathematics, Yuzuzncu Yil University, as an Assistant Professor and an Associate Professor. He is currently working as a Professor and the Head of the Department of Econometrics, Yuzuzncu Yil University. He gives invited talks on a lot of symposium and conferences held at the international level. He has published more than 20 articles in international journal with highly impact factors. His research interests include stiff differential equations, singular perturbation problems, difference equations, delay differential equations, and fractional differential equations.

MUHAMMAD REAZUL HAQUE (Member, IEEE) received the B.Sc.Engg. degree in computer science and engineering from Queens University, Dhaka, Bangladesh, the M.Sc.Engg. degree (Hons.) in computer systems engineering from the University of East London (UEL), U.K., in 2013. He is currently pursuing the Ph.D. degree by research in information technology with Multimedia University, Malaysia. He enlisted as a Young Scientist and a Researcher by Science and ICT Ministry of Bangladesh for the project Auto Fire Protector System. From 2014 to 2015, he worked as a Senior Software Programmer with Axcell Pte. Ltd., Singapore. He joined as a Research Scholar with Multimedia University for the project of Telekom Malaysia Research and Development Sdn. Bhd. (TM R&D), in December 2016. He has published many research articles in IEEE conferences, international journals, two patents, and several book chapters by Springer International Publishing AG, Switzerland, USA, and Singapore, Part of Springer Nature. His research interests include software defined networking, satellite communication, network security, DDoS attack, unmanned aerial vehicles, electric vehicles, artificial intelligence, robotics, and mathematical programming. He received the Gold Medal from Dr. Muhammad Monjurul Islam Siddiquee Sir for the project The Great Thought Reflects (Mohavabna Protibimba). He has been serving as a Reviewer for many IEEE TRANSACTIONS ON INDUSTRIAL INFORMATICS, IEEE/ACM TRANSACTIONS ON NETWORKING, IEEE ACCESS, and *IET Networks*.

JOEL J. P. C. RODRIGUES (Fellow, IEEE) is currently a Professor with the Federal University of Piauìì, Brazil, and a Senior Researcher with the Instituto de Telecomunicacoes, Portugal. He is a collaborator of the Postgraduation Program on Teleinformatics Engineering with the Federal University of Cearaì (UFC), Brazil. He is also the Leader of the Next Generation Networks and Applications (NetGNA) Research Group (CNPq). He has authored or coauthored over 950 articles in refereed international journals and conferences, three books, two patents, and one ITU-T Recommendation. He is a member of the Internet Society and a Senior Member of ACM. He received several outstanding leadership and outstanding service awards from the IEEE Communications Society and several best papers awards. He is an IEEE Distinguished Lecturer, a Member Representative of the IEEE Communications Society on the IEEE Biometrics Council, and the President of the Scientific Council at ParkUrbis–Covilha Science and Technology Park. He was the Director of the Conference Development—IEEE ComSoc Board of Governors, the Technical Activities Committee Chair of the IEEE ComSoc Latin America Region Board, the past Chair of the IEEE ComSoc Technical Committee on eHealth and the IEEE ComSoc Technical Committee on Communications Software. He was a Steering Committee Member of the IEEE Life Sciences Technical Community, and the Publications Co-Chair. He is also the Editor-in-Chief of the *International Journal of E-Health and Medical Communications* and an editorial board member of several high-reputed journals. He has been the General Chair and the TPC Chair of many international conferences, including IEEE ICC, IEEE GLOBECOM, IEEE HEALTHCOM, and IEEE LatinCom.

DANDA B. RAWAT (Senior Member, IEEE) received the Ph.D. degree from Old Dominion University, Norfolk, VA, USA. He is currently a Full Professor with the Department of Electrical Engineering and Computer Science (EECS), the Founder and the Director of the Data Science and Cybersecurity Center, Howard University, the Director of Cyber-security and Wireless Networking Innovations (CWiNs) Research Laboratory, the Graduate Program Director of Howard-CS Graduate Programs, and the Director of the Graduate Cybersecurity Certificate Program, Howard University, Washington, DC, USA. He is involved in research and teaching in the areas of cybersecurity, machine learning, big data analytics and wireless networking for emerging networked systems including cyber-physical systems, the Internet of Things, multi domain battle, smart cities, software defined systems, and vehicular networks. His professional career comprises more than 18 years in academia, government, and industry. He has secured over $16 million in research funding from the U.S. National Science Foundation (NSF), the U.S. Department of Homeland Security (DHS), the U.S. National Security Agency (NSA), the U.S. Department of Energy, the National Nuclear Security Administration (NNSA), DoD Research Labs, Industry (Microsoft, Intel, and so on), and private foundations. He has delivered over 20 keynotes and invited speeches at international conferences and workshops. He has published over 200 scientific/technical articles and ten books. He has served as a Technical Program Committee (TPC) Member for several international conferences, including IEEE INFOCOM, IEEE GLOBECOM, IEEE CCNC, IEEE GreenCom, IEEE ICC, IEEE WCNC, and IEEE VTC conferences. He is also a member of ASEE and AAAS, a Senior Member of ACM, and a Fellow of the Institution of Engineering and Technology (IET). He was a recipient of the NSF CAREER Award, in 2016, the Department of Homeland Security (DHS) Scientific Leadership Award, in 2017, the Researcher Exemplar Award 2019 and the Graduate Faculty Exemplar Award 2019 from Howard University, the U.S. Air Force Research Laboratory (AFRL) Summer Faculty Visiting Fellowship, in 2017, the Outstanding Research Faculty Award (award for excellence in scholarly activity) at GSU, in 2015, and the Best Paper Awards (IEEE CCNC, IEEE ICII, BWCA) and Outstanding Ph.D. Researcher Award, in 2009. From 2013 to 2017, he has also served as a Vice Chair of the Executive Committee of the IEEE Savannah Section. He has been serving as an Editor/Guest Editor for over 50 international journals, including an Associate Editor for IEEE TRANSACTIONS ON SERVICE COMPUTING, an Editor for IEEE INTERNET OF THINGS JOURNAL, an Associate Editor for IEEE TRANSACTIONS ON NETWORK SCIENCE AND ENGINEERING, and a Technical Editor for IEEE NETWORK. He has been in Organizing Committees for several IEEE flagship conferences, such as IEEE INFOCOM, IEEE CNS, IEEE ICC, and IEEE GLOBECOM.